ESTIMATING THE LIMITS OF INFILTRATION IN THE URBAN APPALCHIAN PLATEAU

by

Sarah M. Lavin

B.S. in Biological Science, SUNY at Buffalo, 2011

B.A. in Geology, SUNY at Buffalo, 2011

Submitted to the Graduate Faculty of the

Dietrich School of Arts and Sciences in partial fulfillment

of the requirements for the degree of

M.S. in Geology and Planetary Science

University of Pittsburgh

2015

UNIVERSITY OF PITTSBURGH

Dietrich School of Arts and Sciences

This thesis was presented

by

Sarah M. Lavin

It was defended on

July 20, 2015

and approved by

Dr. Charles E. Jones, Lecturer, Department of Geology and Planetary Science

Josef P. Werne, Associate Professor, Department of Geology and Planetary Science

Thesis Director: Daniel J. Bain, Assistant Professor, Department of Geology and Planetary Science

ESTIMATING THE LIMITS OF INFILTRATION IN THE URBAN APPALCHIAN PLATEAU

Sarah M. Lavin, M.S.

University of Pittsburgh, 2015

Urban regions with large areas of impervious cover generate high volumes of surface runoff during wet weather, overwhelming antiquated sewer infrastructure and causing overflow into receiving waters. Green infrastructure in urbanized areas commonly uses infiltration systems to convey surface runoff from impervious surfaces into surrounding soils, which helps mitigate the amount of stormwater entering sewer systems. However, the use of infiltration as a sustainable solution can be limited in regions with unsuitable environmental conditions that can lead to rapid degradation of infiltration systems. Two case studies conducted in Allegheny County, PA that look at the limits of infiltration from excessive stormwater loading and unfavorable soil water dynamics are presented. The first study used infiltration rates and precipitation data to model effective precipitation rates of various storm events over increasing levels of imperviousness in order to characterize local impervious cover thresholds. It was found that local soils are unable to effectively infiltration stormwater from a majority of storm events in regions with greater than 60% imperviousness. These regions would be considered less suitable for the use of infiltration-based green infrastructure and would likely require augmentation with other stormwater management strategies. The second study characterized subsurface soil water dynamics along two hillslopes sites where infiltration-based green infrastructure was installed. Prior to installation, soil moisture was monitored continuously at various depths, and the resulting records were then compared to precipitation data to quantify soil water responses to storm

events. Prevailing expectations of hillslope soil water dynamics assume well-drained profiles and top-down/horizontal wetting front following storm events, even for clay-rich soils like those found in Allegheny County. However, the study sites often underwent inverted wetting during storm events (bottom to top) and displayed relatively slower drainage rates throughout the soil profile, which led to uncharacteristically high soil moisture conditions. These detailed analyses show that unexpected patterns in soil water dynamics exist which could potentially degrade green infrastructure effectiveness. The findings from these two studies suggest that continuous pre-installation monitoring of hydrological conditions and characterization of region-specific impervious cover thresholds is essential to determine proper placement and design of infiltration-based green infrastructure for optimum performance.

TABLE OF CONTENTS

LIST OF TABLES

LIST OF FIGURES

1.0 INTRODUCTION

1.1 HYDROLOGICAL IMPACTS OF URBANIZATION

Urban landscapes are characterized by the construction of impervious surfaces from buildings and transportation infrastructure that replaces natural, pervious land cover (Barbosa et al., 2012; Jacobson, 2011). These surfaces act as physical barriers preventing precipitation from infiltrating into underlying soils, which reduces subsurface flow and greatly enhances surface runoff during wet weather events (Moglen and Kim, 2007; Shuster et al., 2005). Because of this, small storm events in urban regions can generate volumes of runoff equivalent to a large storm event under natural conditions (Shuster et al., 2005). The development of proportionally larger expanses of impervious cover across urban catchments has been known to lead to dramatic changes in local hydrologic flow regimes since the late 1800's, but research in the field didn't become prominent until the 1960's (Moglen and Kim, 2007). Early studies showing the hydrological implications of urbanization noted changes to surface water hydrographs (Leopold, 1968), increased flood events (Anderson, 1970; Hollis, 1975), morphological degradation of stream channels (Hammer, 1972; Wolman, 1967), and stream ecological degradation (Klein, 1979). These changes are all the result of increased volumes of surface runoff that rapidly discharge to waterways during wet weather (Schueler, 1994). Increased surface runoff causes surface hydrographs to have increased storm responses (Rose and Peters, 2001), increased peak flow (Burns et al., 2005), and increased

flashiness, which describes how quickly flow volume changes during a storm event (McMahon et al., 2003). The sudden, flashy pulses of stormwater runoff in streams cause accelerated erosion of channel banks and destruction of aquatic habitats (Booth et al., 2002; Walsh et al., 2005). These effects are greatly amplified in regions with highly concentrated, contiguous impervious cover such as those in densely urbanized cities, commercial, and industrial zones (Burns et al., 2005; Shuster et al., 2005), but even low levels of impervious cover (10-15%) have led to observable degradation of nearby streams (Klein, 1979). Because impervious cover is a primary driver of hydrological changes and is easily quantifiable, the estimation of total or percent impervious cover within watersheds is commonly used to characterize the impacts of urbanization on local waterways (Arnold and Gibbons, 1996; Schueler, 1994).

As urban regions continued to develop, there was a need for more rapid conveyance of surface runoff away from impervious surfaces in order to mitigate flooding (Leopold, 1968). The development of extensive sewer drainage systems, which are collectively referred to as 'grey infrastructure', allow for more efficient transport of stormwater away from source areas (Arnold Jr and Gibbons, 1996; Walsh et al., 2005) (Figure 1.1). Before the 1900's, most cities constructed combined sewer systems that accepted both wastewater (domestic, commercial, and industrial) and stormwater into one piped network (EPA, 2004). The single stream of sewer and stormwater would be discharged into local waterways through outfall pipes before treatment plants were present (Figure 1.1a). However, the repeated delivery of waste into receiving waters had detrimental effects on water quality and caused outbreaks of water-borne diseases downstream of sewer inputs (EPA, 2004). This led to a shift towards separate sewer systems where wastewater and stormwater were each channeled into separate pipe networks (Figure 1.1b). After the 1900's, the wastewater in separate sewer systems was diverted to a waste

treatment facility, and stormwater overflows from pipe outfalls directly into receiving waters. The existing combined sewer systems were also connected to pipes flowing to treatment facilities, but still continue to overflow into local waterways during wet weather events when the facility or pipe capacity is exceeded (Figure 1.1a).

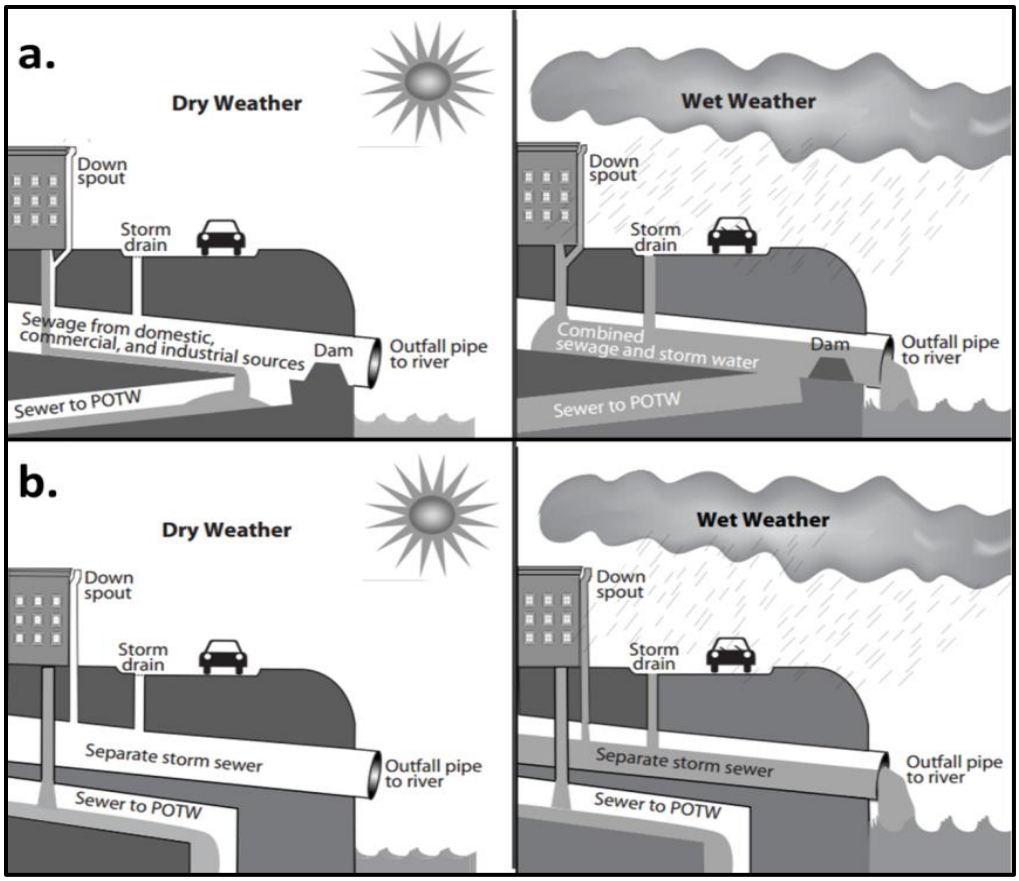

Figure 1.1: Types of sewer systems. Combined **(a)** and separate **(b)** storm sewer systems function differently during wet and dry weather due to differences in design. Image courtesy of the US Environmental Protection Agency (2004).

Combined sewer overflows (CSO's), containing both wastewater and stormwater, deliver water-borne pathogens, organic pollutants, oxygen-depleting compounds, metals, and sediments directly into receiving waters, creating negative impacts on environmental and public health (Curriero et al., 2001; EPA, 2004; Field and Struzeski, 1972; Gasperi et al., 2010). Separate

storm sewers do not carry wastewater to local waterways, but storm sewer overflows (SSO's) from these drainage systems can also cause significant impacts on water quality (EPA, 2004). Sediments and contaminants from urban land use and anthropogenic activities collect on impervious surfaces and are washed into storm sewers with runoff during wet weather events (Moglen and Kim, 2007; Schueler, 1994) and are discharged into local streams. CSO waters generally contain higher percentages of organics, nutrients and pathogens from waste contributions, whereas SSO waters contain higher percentages of metals from anthropogenic activities (Clark et al., 2007). An increased number of overflow events from both sewer systems is associated with increases in water quality issues for receiving waters (EPA, 2004).

There are a number of environmental factors that can lead to increases in the volume and number of overflow events from both combined and separate sewer systems. Large storm events resulting in high volumes of stormwater will overwhelm sewer systems and lead to overflow events (Roy and Shuster, 2009); however even small storm events can generate volumes of runoff large enough to overwhelm systems in regions with high percent impervious cover (Fletcher et al., 2013). Separate sewer systems are not designed to transport the large volumes of stormwater that combined systems can manage, so these sewers are subject to more numerous overflow events (EPA, 2004). Also, when combined and separate sewer systems reach capacity before waters have a chance to discharge at outfall pipes, wastewater and stormwater can back-up into buildings and escape through utility access covers causing localized flooding (EPA, 2004). Lastly, high levels of baseflow in sewers decrease pipe capacity, leading to more numerous outflow events during wet weather (Broadhead et al., 2013). Increased baseflow is

primarily caused by the burial of streams and springs into sewer systems during urban expansion (Barbosa et al., 2012; Broadhead et al., 2013) and by groundwater seepage into cracked sewer pipes (Fletcher et al., 2013).

As urbanization continues, the issues with current stormwater drainage systems will likely be amplified by increases in impervious cover (Semadeni-Davies et al., 2008) and the deterioration of aging infrastructure (Kaushal and Belt, 2012), leading to more overflow events and decreased quality of local waterways.

1.2 STORMWATER ISSUES IN ALLEGHENY COUNTY, PA

The City of Pittsburgh and its metropolitan area, located in Allegheny County, Pennsylvania, are serviced by both sanitary and combined sewer systems, many of which were constructed in the early 1900's (Tarr, 2004). The city is located at the confluence of the Allegheny and Monongahela Rivers into the Ohio River, all of which are directly connected to local sewer systems through 258 combined sewer outfalls and 52 sanitary sewer outfalls, more than any other city in the United States (ALCOSAN, 2008; Tarr, 2004). Total overflow volumes from these outfalls have been estimated to discharge approximately 9.6 billion gallons of sewer overflow annually, with 8.3 million gallons being from combined sewers alone (ALCOSAN, 2008). The primary contaminants from overflow events include fecal coliform bacteria, phosphorus, and suspended solids (ALCOSAN, 2008). The sewer systems are antiquated and suffer from structural degradation and enhanced baseflow from groundwater seepage and buried streams (Tarr, 2004). In 2008, local sewer authorities were issued consent decrees from state and

federal agencies requiring the improvement of existing conditions in order to comply with the Clean Water Act and PA Clean Streams Law (PWSA, 2013). In response, the local authorities created wet weather plans with goals to eliminate overflow events from sanitary sewers and significantly decrease events from combined sewers. Proposals suggest reaching the goals by building new infrastructure and detention facilities within the sewer network and increasing wet weather capacities at treatment facilities (ALCOSAN, 2008). However, the installation of large storage structures takes up much-needed space in the urban landscape, and the construction and continuous maintenance of sewer infrastructure will be very costly (Kaushal and Belt, 2012; Mikkelsen et al., 1996). This is why the EPA and Pittsburgh Water and Sewer Authority (PWSA) have suggested that the City of Pittsburgh takes a combined approach towards better stormwater management by including improvements to grey infrastructure and the development of more natural, cost-effective green infrastructure into wet weather plans (PWSA, 2013).

1.3 GREEN INFRASTRUCTURE

With recent concerns about the sustainability of conventional grey infrastructure, efforts have turned towards implementing more natural stormwater management practices to help reduce surface runoff entering sewer systems and mitigate pollutant loads entering local waterways (Barbosa et al., 2012; Mikkelsen et al., 1996). These efforts can be accomplished through either non-structural (forest conservation, minimizing landscape disturbance, street cleaning) or structural means (Barbosa et al., 2012, PADEP, 2006). Structural stormwater management practices are collectively referred to as green infrastructure in this study, but they have also been

known as low-impact development (LID) strategies, structural best management practices (BMP's), or water sensitive urban design (WSUD) (Burns et al., 2012; Roy and Shuster, 2009). The structures are designed to capture and retain surface runoff to control the timing and volume of stormwater reaching sewers and local waterways with the goal of reducing the volume and number of storm sewer overflows (Barbosa et al., 2012; EPA, 2004). Green infrastructure has proved to be a viable alternative to conventional sewer drainage systems and has been shown to improve downstream water quality, channel stability, and stream ecology (Fletcher et al., 2013; Loperfido et al., 2014; Roy and Shuster, 2009). The structures can also contribute to the mitigation of storm sewer overflow (Broadhead et al., 2013; Mikkelsen et al., 1996), and have considerable social and economic benefits over grey infrastructure (Barbosa et al., 2012; PWSA, 2013).

The earliest forms of green infrastructure used retention techniques to reduce peak flow by temporarily capturing stormwater in constructed dry basins and detention ponds, where it would be released slowly into waterways (Holman-Dodds et al., 2003). These structures were typically centralized with a few large structures located at or near stream channels at the end of sewer networks (Loperfido et al., 2014; Williams and Wise, 2006). The suspended solids and pollutants in the stormwater have time to settle out at the bottom of the detention structure before the water is released into streams (Barbosa et al., 2012). However, this form of green infrastructure has only been effective in reducing storm sewer overflows for large storm events and thus has minimal impact on solving hydrological issues, so strategies have opted instead for the use of more distributed, infiltration-based green infrastructure for stormwater mitigation (Loperfido et al., 2014; Mikkelsen et al., 1996).

Infiltration-based green infrastructure is installed close or next to impervious surfaces and is designed to capture surface runoff closer to the source to allow for the slow release of water into surrounding soils via infiltration. These systems can be distributed throughout a catchment in order to disconnect impervious surfaces from sewers and convey the surface runoff into surrounding soils instead (Holman-Dodds et al., 2003). There are various types of infiltration-based green infrastructure, each with different advantages, and include things such as infiltration trenches, vegetated swales, rain gardens, and pervious pavement (Figure 1.2). Each type is connected directly to adjacent impervious surfaces, and receives stormwater either concentrated through a dedicated inlet like in rain gardens and infiltration trenches, or distributed over its surface like with vegetated swales and pervious pavement. Infiltration trenches rely almost entirely on subsurface hydraulics to redistribute stormwater, but swales and rain gardens have the added benefits of evapotranspiration from vegetation to help redistribute water (Hamel et al., 2013). Each structure type can have added storage in the form of gravel or aggregate beds, or can have underdrains and overflow pipes for excessive inputs. The structure size and design is decided during the planning phase to estimate hydrologic needs (Hamel et al., 2013; PADEP, 2006).

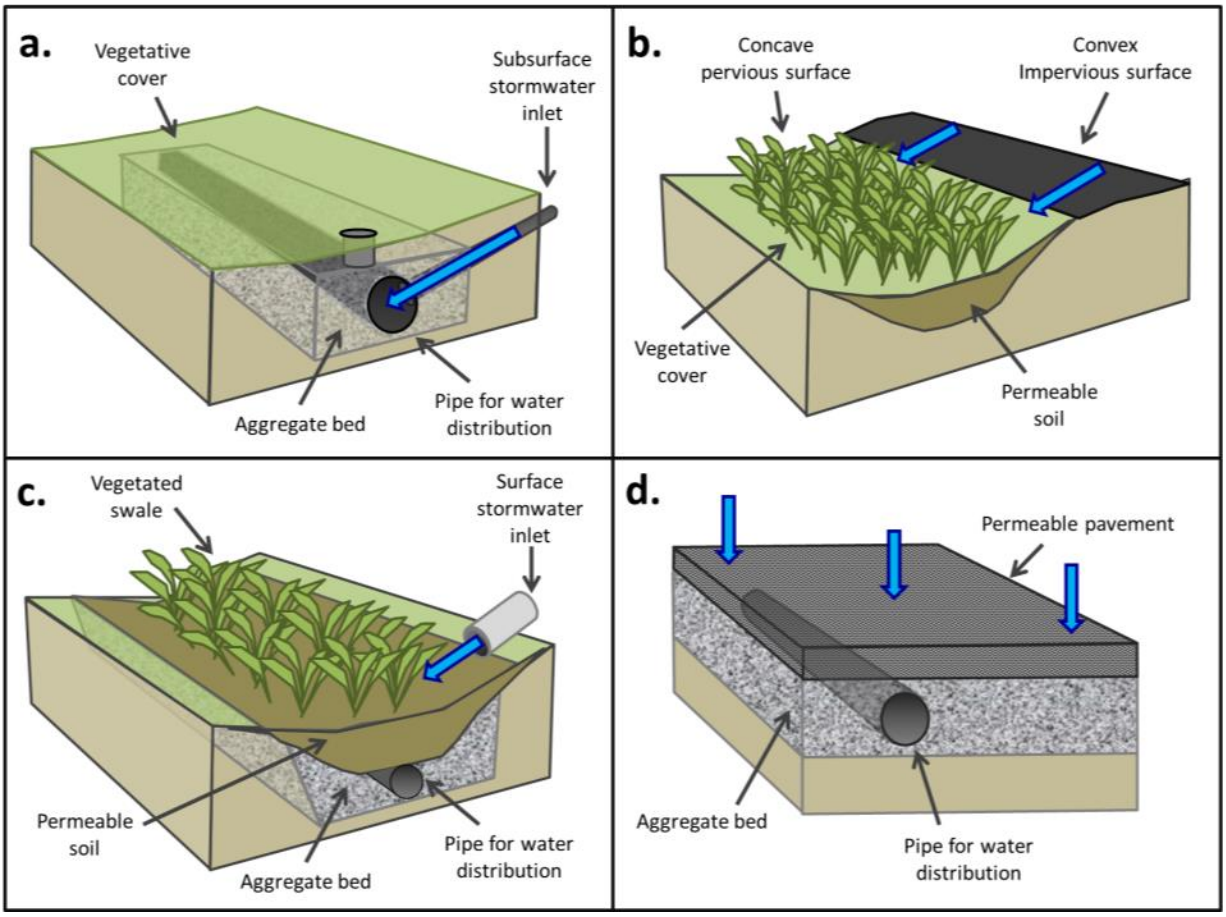

Figure 1.2: Types of infiltration-based green infrastructure: **(a)** infiltration trench, **(b)** vegetated swale, **(c)** rain garden, and **(d)** pervious pavement. Blue arrows represent flow paths of stormwater into the infiltration system.

The process of allowing stormwater to infiltrate into soils and connect with subsurface hydraulic processes more closely mimics natural conditions. Infiltration-based green infrastructure can help mitigate the negative impacts of traditional stormwater systems, especially for smaller and more numerous storm events where detention techniques have been ineffective (Loperfido et al., 2014). There is also an added benefit of pollutant removal through filtration of stormwater through the surrounding soils (Fletcher et al., 2013; Hamel et al., 2013). When properly implemented, the structures have been shown to decrease surface runoff, mitigate storm sewer overflows, and promote groundwater recharge (Dietz, 2007; Holman-Dodds et al., 2003; Mikkelsen et al., 1996).

1.4 LIMITS OF INFILTRATION-BASED GREEN INFRASTRUCTURE

Although infiltration technology has great potential for stormwater mitigation, the benefits and functionality of these systems are dependent on its design and environmental factors at the installation site. The climate, geology, hydrology, drainage area, and total impervious cover should all be considered before choosing to install infiltration-based green infrastructure (Barbosa et al., 2012; Gilroy and McCuen, 2009; Hamel et al., 2013). Infiltration devices cannot recover storage capabilities if stormwater cannot be infiltrated quickly; therefore, their functionality relies on efficient subsurface drainage of stormwater within adjacent soils (Shuster et al., 2007; Williams and Wise, 2006). Hydrologic failure occurs when infiltration is inhibited from low soil permeability or when soil water storage capacity is limited from shallow groundwater tables, high antecedent soil moisture conditions, or shallow depths to bedrock

(Bouwer, 2002; Hood et al., 2007; Shuster et al., 2007; Williams and Wise, 2006). In addition, conveying runoff volumes from large areas of impervious cover into pervious surfaces can be difficult when infiltration is low or there is little room to accept high water volumes (Holman-Dodds et al., 2003). The area of directly connected impervious surfaces has observable impacts on the amount of runoff mitigated by infiltration structures, with runoff reductions from infiltration being lowest in densely urbanized areas (Barbosa et al., 2012; Brander et al., 2005). These regions also have higher contaminant loads that can be washed into infiltration devices with stormwater and can potentially lead to groundwater contamination (Pitt et al., 1999; Weiss et al., 2008). Water directly fed into the subsurface, such as with infiltration trenches, bypasses the organic soil layer and root zone where most pollution filtration occurs, and poses a greater risk of groundwater contamination (Mikkelsen et al., 1996). Stormwater can also carry sediments and other suspended solids into infiltration devices which can decrease hydrologic function over time due to clogging (Fletcher et al., 2013; Le Coustumer et al., 2009; Reddi et al., 2000). Initial hydraulic conductivity of surrounding soils determines the rate of failure, with lower permeable soils decreasing the lifespan of infiltration-based green infrastructure (Le Coustumer et al., 2009; Warnaars et al., 1999).

Without proper planning or adequate knowledge of local environmental factors, infiltration devices intended for mitigating stormwater runoff can ultimately experience premature hydrologic failure and decreased lifespans due to clogging and unfavorable hydrological conditions. Proper planning can aid in understanding the structure's effect on subsurface flow and thus its long-term hydrological function, but little attention is given to this subject in current literature (Hamel et al., 2013). Planning and evaluation varies across catchments, and lack of knowledge and data gaps can make the design and implementation of

infiltration-based green infrastructure problematic, leading to poor decisions in stormwater management practices (Barbosa et al., 2012). In this document, we present two studies aimed at identifying the limits of infiltration-based green infrastructure in urban regions of the Appalachian plateau physiographic province with case studies in Allegheny County, Pennsylvania, using knowledge of impacts from impervious surfaces and local hydrological regimes.

2.0 STUDY 1: CHARACTERIZING IMPERVIOUS COVER THRESHOLDS

2.1 BACKGROUND AND RESEARCH AIMS

The wet weather plan for Allegheny County will implement infiltration-based green infrastructure throughout the region with the goal of reducing impervious surface runoff flows into combined sewer systems. The function of these structures will depend on design and environmental factors, such as soil physical properties and the area of impervious cover draining into the system (Hamel et al., 2013). When infiltration rates of adjacent soils are low or when the volume of water input is high, the structures will not be able to redistribute all stormwater inputs into the subsurface, and instead the pervious surface will just contribute to runoff generation (Hamel et al., 2013; Williams and Wise, 2006). This study uses percent impervious cover to estimate true values of water input rates during various storm events and evaluates the ability of soils in to infiltrate these inputs. Understanding these processes can aid decisions on green-infrastructure placement in the county based on whether or not site conditions will negatively impact their hydrological function. In a case study of Allegheny County, this research looks to answer the following questions: (1) is there a limitation to infiltration in Allegheny County relative to increasing impervious cover, and, (2) what are the implications for green infrastructure built in threshold areas?

2.2 METHODS

2.2.1 Regional Description

Allegheny County is located in south-western Pennsylvania and has a humid continental climate, with an average annual temperature of 10°C and average annual rainfall of 96.5 centimeters. Winters are cold (2°C average temperature) and wet, and summers are warm (22°C average temperature) and slightly drier (NWS, 2013). The region is part of the Appalachian Plateau physiographic province. The surface rocks are primarily Pennsylvanian in age (approximately 300-320 million years old), and are made up of nearly-horizontal, interbedded layers of shale, siltstone, sandstone, and limestone. Topographic relief varies considerably across the landscape which is composed of flat-topped ridges and steeply sloping valley walls (Wagner, 1970). The upland and hillslope soils are typically well-drained colluvial silt loams and silty-clay loams, categorized as Gilpin-Upshur complex soils. Valley areas contain poorly drained silt-loams with shallow water-tables (Newbury et al., 1981). The county lies entirely within the Ohio River drainage basin. Two of its largest rivers, the Allegheny and Monongahela Rivers, join to form the Ohio River at the center of the county in Pittsburgh, the county's largest city and the second largest city in Pennsylvania (Barnes and Sevon, 1996).

2.2.2 Soil Infiltration Rates

The distribution of soil infiltration rates in Allegheny County was characterized by compiling field measurements, local measured values (Kirk, 2014), and information from the NRCS Soil Survey national database (Soil Survey Staff, 2014). Infiltration rates were measured using a double-ring infiltrometer (30.5cm outer ring, 15.25cm inner ring) within an urban park in

Pittsburgh, PA. Measurements were made along three transects spanning forest/open space boundaries to collect infiltration rates from lawns, forests, and forest edges. Protocols for measurement followed the "Methodology for Double-Ring Infiltrometer Field Test" as described in Appendix C of the Pennsylvania Stormwater Best Management Practices Manual (PADEP, 2006). Infiltration rates are dynamic and change as a function of water input rates, slope of the landscape, and antecedent soil moisture content (Nassif and Wilson, 1975). Double-ring infiltrometers are designed to reduce effects of lateral flow caused by sloped soils and pore pressure from dry conditions while taking measurements. After hammering the infiltrometer 2 inches into the soil, both rings were filled with tap water and allowed to infiltrate for 30 minutes to saturate the ground, refilling the rings when necessary. During this time, water in the outer ring flows through the soil both laterally and vertically and buffers the movement of water infiltrating from the inner ring. This means that any water permeating through the soil from the inner ring will be forced to move vertically, yielding measurements of infiltration rates that excludes lateral movement (Figure 2.1) (Dingman, 1994).

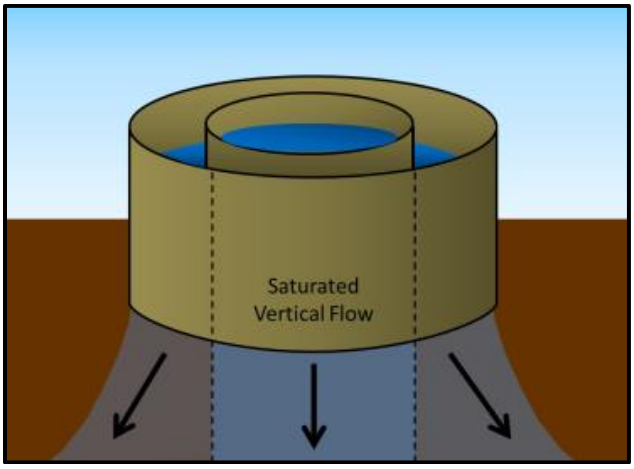

Figure 2.1: Hydrologic function of a double-ring infiltrometer. Water infiltrating from the outer rings moves both laterally and vertically, but only vertical flow occurs in the inner ring where infiltration measurements are made from.

After this step, both rings were filled completely, and the drop in water level within the inner ring was recorded at 10 minute intervals (or 3 minute intervals for sites with faster infiltration), refilling when necessary to maintain a steady water input. As soils reach saturation, the infiltration rates reach a steady state. These steady state measurements were averaged to yield a final value for infiltration rate. This rate is representative of the soil infiltration capacity under saturated conditions (Dingman, 1994). Local reported values of infiltration rate were also measured using double-ring infiltrometer.

Infiltration rates of soils in Allegheny County were also compiled from the NRCS Soil Survey (Soil Survey Staff, 2014). Values of surficial saturated hydraulic conductivity (K_{sat}) were found for each soil group present in the county and used as a proxy for infiltration rates. The K_{sat} of surface soils is approximately equivalent to the infiltration capacity at saturation (Dingman, 1994), which is the exact measurement yielded by field methods. Since K_{sat} values in the Soil Survey are given in a range for any given soil group, this range was averaged to yield a measure of infiltration rate.

2.2.3 Plot Analysis of Impervious Cover

The distribution of percent impervious cover across Allegheny County was measured using geospatial sampling. Four transects were drawn between downtown Pittsburgh and the county line in each cardinal direction. Each transect was split into 8-10 segments of equal length and points were randomly placed along these segments to provide a stratified random sample of locations along the urban to rural gradient (Figure 2.2).

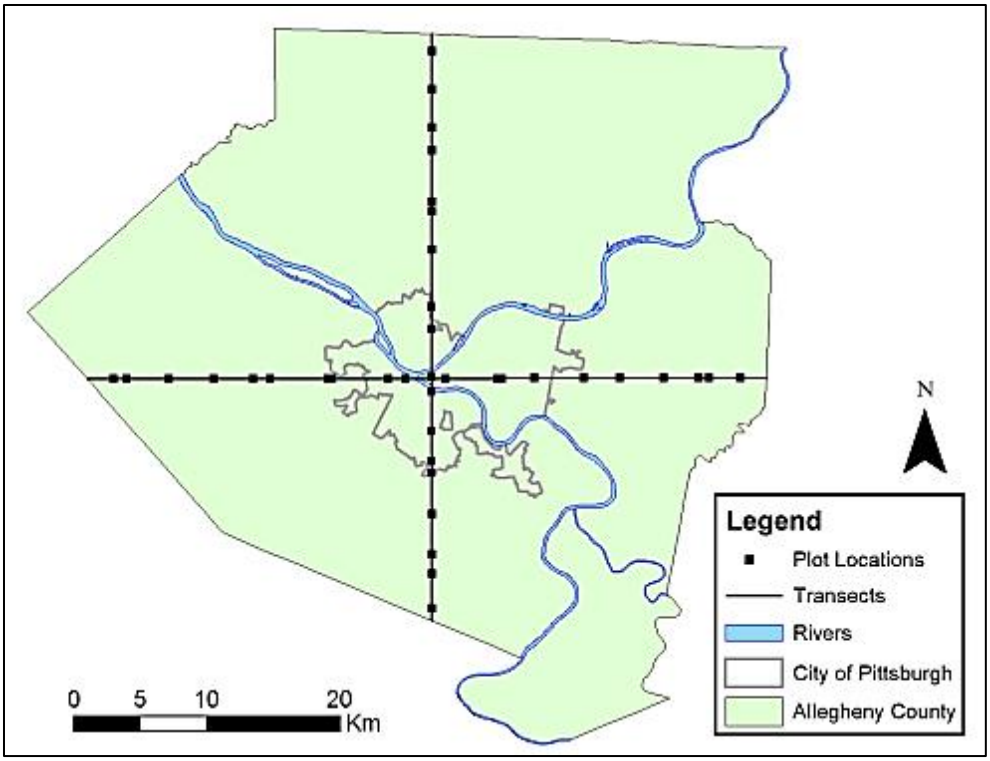

Figure 2.2: Transect and analysis plot locations across Allegheny County. Each transect starts in downtown Pittsburgh and extends to the county border. Geospatial data was obtained from PA Spatial Database Access (PASDA, 2013). The thirty-eight plots are represented by the black points.

A feature envelope was created based on a 100m buffer to generate 200m x 200m analysis plots for each sampling point. Impervious surfaces within the analysis windows were identified as streets, buildings, driveways, parking lots, and sidewalks (Allegheny County, 2006, 2013a). Parking lots, sidewalks and driveways were digitized into polygon features using aerial orthoimagery with 1 ft. pixel resolution (Allegheny County, 2013b). All polygon features were merged and the combined area of these surfaces within each individual window was calculated to yield percent impervious cover (Figure 2.3).

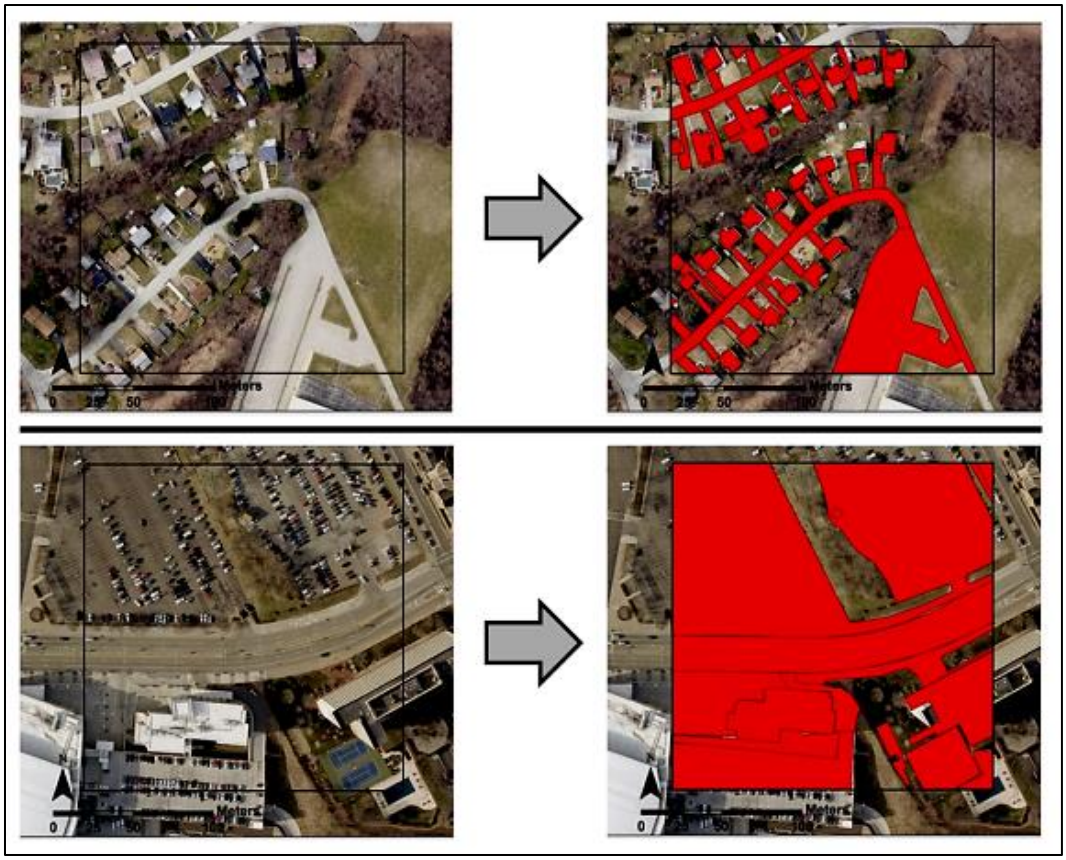

Figure 2.3: Impervious cover characterization. The maps show aerial orthoimagery (left) and digitized polygons of impervious surfaces (right) within two example plots. Geospatial data was obtained from the PA Spatial Database Access (PASDA, 2013).

2.2.4 Effective Precipitation Calculations

Precipitation data was obtained from the National Weather Service's Precipitation Frequency Data Server (PFDS) for Pittsburgh, PA. PFDS storm events were given as rainfall totals, but average rainfall rates were calculated by dividing these values by the duration of the storm.

For the purpose of this study, it was assumed that all precipitation falling on impervious surfaces would runoff completely into adjacent pervious surfaces. Therefore, these pervious surfaces are experiencing water inputs from an effectively larger storm event, and so the amount of rainfall falling on pervious surfaces plus any additional water from runoff is considered together as effective precipitation (Figure 2.4).

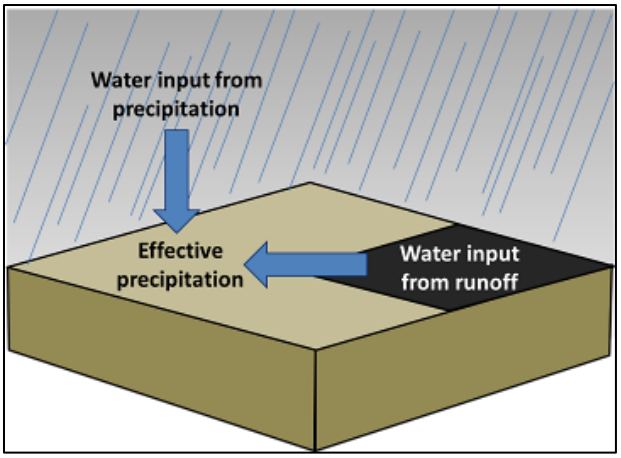

Figure 2.4: Water inputs to pervious surfaces. Effective precipitation changes with storm size and the percent impervious cover.

The effective precipitation was calculated for each storm event for regions with varying percent impervious cover using the following equation:

$$P_{eff} = P \times \left(\frac{1}{1 - \%IC}\right)$$

where P_{eff} is effective precipitation, P is the storm's rainfall rate, and %IC is percent impervious cover. The resulting values were then compared to average infiltration rates to find impervious cover thresholds where effective precipitation rates would produce surface runoff.

2.3 RESULTS

2.3.1 Infiltration Rate Threshold

Infiltration rates were compiled from national databases, local resources, and field measurements to create a distribution of infiltration rates for Allegheny County. The average infiltration rate was 1.05 mm/min with a standard deviation of 1.69 mm/min, and the median value was 0.55

mm/min (Figure 2.5). This large standard deviation is due to the log-normal distribution of the data, with a bulk of the data (>95%) occurring between 0.05 – 3.00 mm/min. A majority of these measures were from Soil Survey data. The large difference between median and average values of the data is caused by weighted influence of a small number of infiltration rate measurements that exceeded 3mm/min. Given this data, the average infiltration rate of 1.05 mm/min was used as a conservative threshold value for the results of effective precipitation (P_{eff}) calculations, and all water input rates above this value were assumed to generate overland flow.

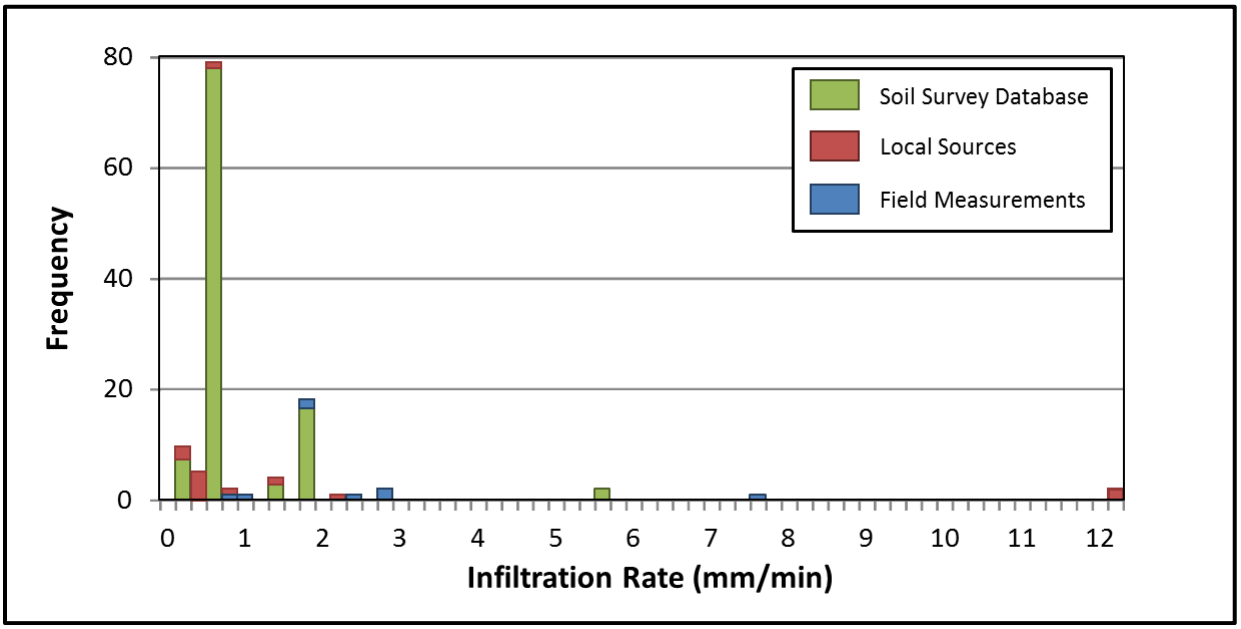

Figure 2.5: Infiltration rate distribution. The graph above is a histogram showing the distribution of infiltration rates from across Allegheny County, with an average infiltration rate of 1.05 mm/min. Data is compiled from national databases and from field measurements that were made in Pittsburgh, PA. The distribution is separated by data source.

2.3.2 Impervious Cover Plot Analysis

A total of thirty-eight plots were analyzed in ArcGIS for percent impervious cover over an urban to rural gradient, representing 0.08% of the total county area (Figure 2.2). The average percent

impervious cover within the analyzed plots was 27%, and the data curve is skewed to the left (Figure 2.6). This skew is caused by a bulk of the data (87%) occurring between 0 – 50% impervious cover. Only five plots contained > 50% impervious cover, and of these, four were within the Pittsburgh city boundary. The percentages with the highest frequency (0%, 15%, 25%, and 30%) were used in the calculation of effective precipitation for a range of local storm events. Higher percentages of impervious cover (50%, 75%, and 90%) were also chosen to represent urban areas.

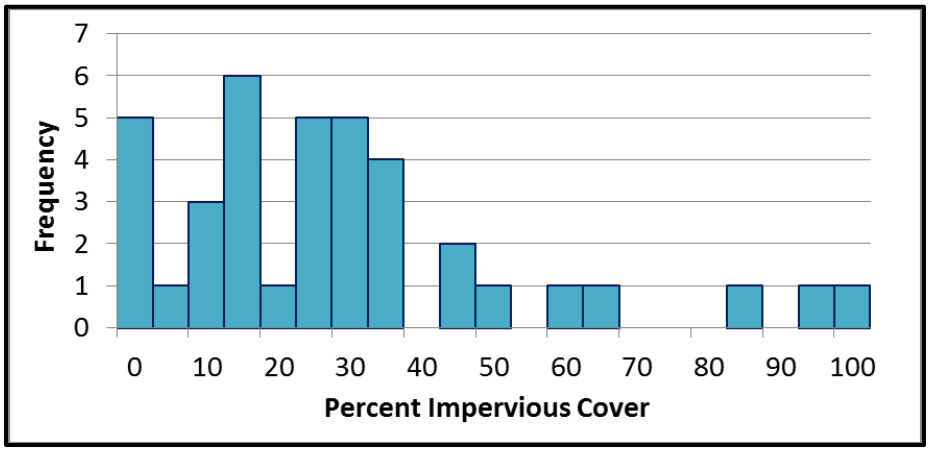

Figure 2.6: Percent impervious cover distribution from plot analysis. A majority of the plots contained less than 40% impervious cover.

2.3.3 Effective Precipitation Analysis

National Weather Service point precipitation frequency analyses for storm events in Pittsburgh, PA were obtained as a matrix containing total rainfall (in inches) for 1, 2, 5, 20, 25, 50, and 100-year storms at various storm durations up to 24-hour storms. Rainfall rates were calculated to represent water input for each storm event in mm/min (Table 2.1). These rates represent the P_{eff}

in regions with 0% impervious cover. These storm events were then modeled to determine the P_{eff} in regions of 15%, 25%, 30%, 50%, 75%, and 90% impervious cover.

Table 2.1: Precipitation data for Pittsburgh, PA obtained from NWS PFDS. The data shows average rainfall rates in millimeters per minutes (mm/min). The highlighted storms are those that exceed a rainfall rate of 1.055 mm/min, and represent the storms above the 0% impervious cover contour line in Figure 2.7.

		Storm Reoccurrence Interval (years)						
		1	2	5	10	25	50	100
Storm Duration (minutes)	5	1.63	1.93	2.34	2.64	3.00	3.30	3.61
	10	1.24	1.50	1.80	2.03	2.31	2.51	2.72
	15	1.02	1.22	1.47	1.66	1.90	2.08	2.25
	30	0.67	0.81	1.01	1.15	1.34	1.48	1.63
	60	0.41	0.50	0.63	0.73	0.87	0.98	1.08
	120	0.23	0.29	0.36	0.42	0.50	0.56	0.63
	180	0.17	0.20	0.25	0.29	0.35	0.40	0.44
	360	0.10	0.12	0.15	0.17	0.21	0.23	0.26
	720	0.06	0.07	0.09	0.10	0.12	0.14	0.15
	1440	0.03	0.04	0.05	0.06	0.07	0.08	0.09

Contour graphs of rainfall rate were generated using the R program package for each impervious cover condition and the threshold value of 1.05 mm/min (R Core Team, 2013). The contours for each impervious cover condition were then combined into a single plot to show the number of storms that exceed threshold values for each condition (Figure 2.7). Each line represents an effective precipitation rate of 1.05 mm/min and varying impervious cover. Areas above the contours represent storms that would lead to runoff generation (Table 2.1). As visualized in Table 2.1, this means that only 25 of the 70 storms analyzed occurred above the 1.05 mm/min contour. The contour plot shows regions with 0% impervious cover can fully infiltrate a majority of analyzed storm events, typically those with storm durations greater than 30 minutes. In general, P_{eff} is relatively insensitive to changes in impervious cover from 0-50%.

Regions with more than 50% impervious cover are less capable of infiltrating rainfall effectively from a majority of storm events, even those with a higher duration; however these areas make up a small proportion of the county (only ~13% of sampled areas). The infiltration rate must increase geometrically in relation to the increasing area of impervious surfaces. The average soil infiltration rate would have to increase four-fold (to 4.22 mm/min) in order to fully infiltrate a rainfall rate equivalent to the threshold value of 1.05 mm/min (approximately the rate of a 1-yr, 15-min storm) in a region with 75% impervious cover (Table 2.2).

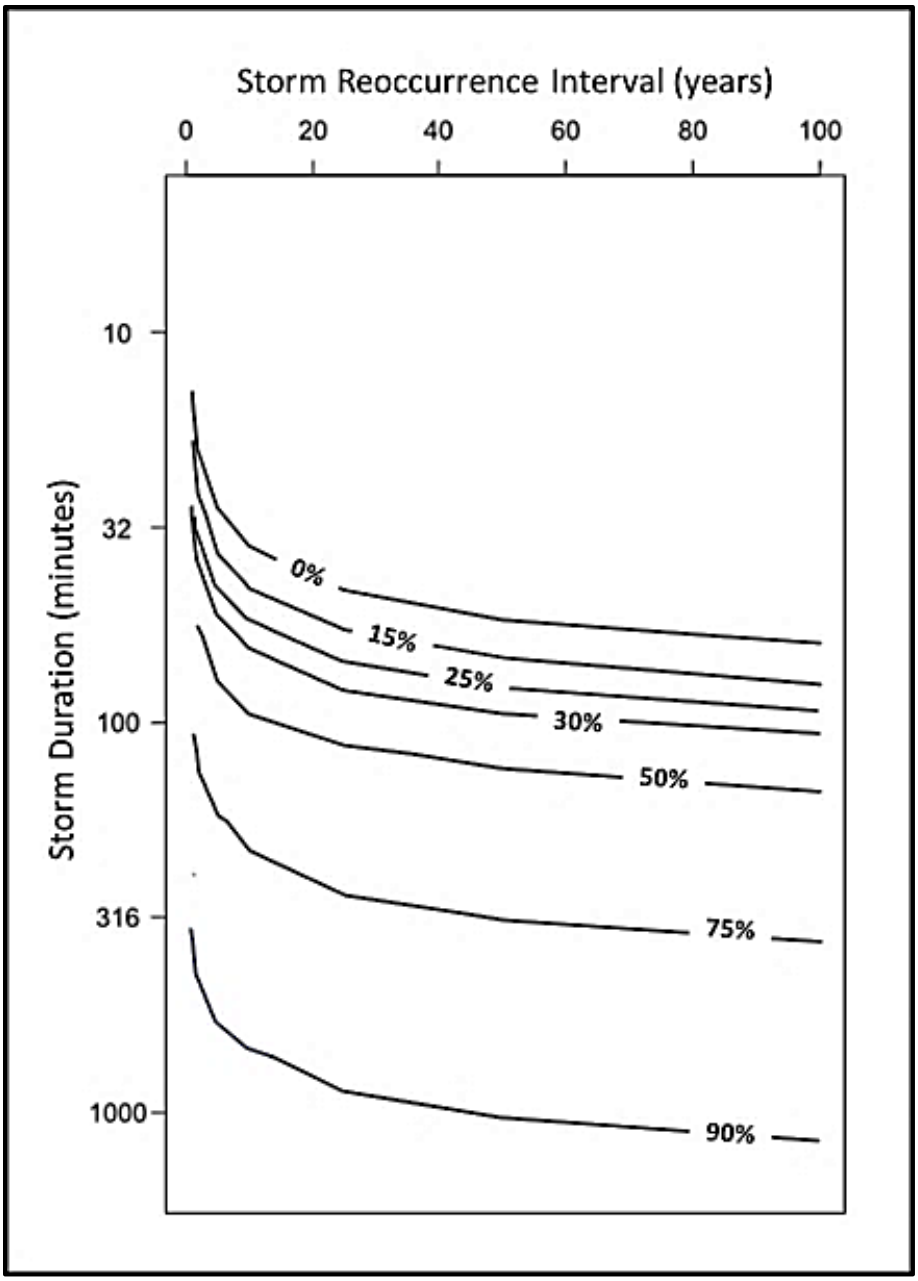

Figure 2.7: Contour graph of infiltration thresholds (P_{eff} = 1.05 mm/min) at varying modelled percent impervious cover. Storm events that lie above an individual contour line are those that would generate runoff in that model. The contour line for 0% impervious cover marks the boundary that is displayed in Table 2.1.

Table 2.2: Percent increase of infiltration rates. This table shows an analysis of percent increase in infiltration rates required to completely infiltrate a 1.05 mm/min storm as the area of impervious cover increases.

Percent Impervious Cover	Required Infiltration Rate (mm/min)	Percent Increase in Infiltration Rate
0%	1.05	0%
15%	1.24	18%
25%	1.40	33%
30%	1.58	50%
50%	2.11	100%
75%	4.22	300%
90%	10.55	900%

Each storm event characterized by NWS's frequency analysis has an impervious cover threshold above which local soils will not be able to infiltrate the effective precipitation, thus generating runoff. Typically, the volume of stormwater captured by green infrastructure in Pennsylvania is calculated using the rainfall amount of a 2-year, 24-hour storm (PADEP, 2006). In Pittsburgh, PA, a 2-year, 24-hour storm has a rainfall rate of 0.04 mm/min. This storm, plus a number of smaller, more frequent storms were modelled to show P_{eff} at increasing values of percent impervious cover to identify the threshold over which local infiltration rates would be exceeded (Figure 2.8). Results show that threshold values are exceeded for a 1-yr, 30-min storm at 37% impervious cover; 1-yr, 1-hr storm at 60%; 1-yr, 2-hr storm at 78%; 1-yr, 6-hr storm at 90%; and 2-yr, 24-hr storm at 96%. The 1-yr, 1-hr storm was used as a standard for geospatial analysis of threshold regions (>60% impervious cover) across Allegheny County.

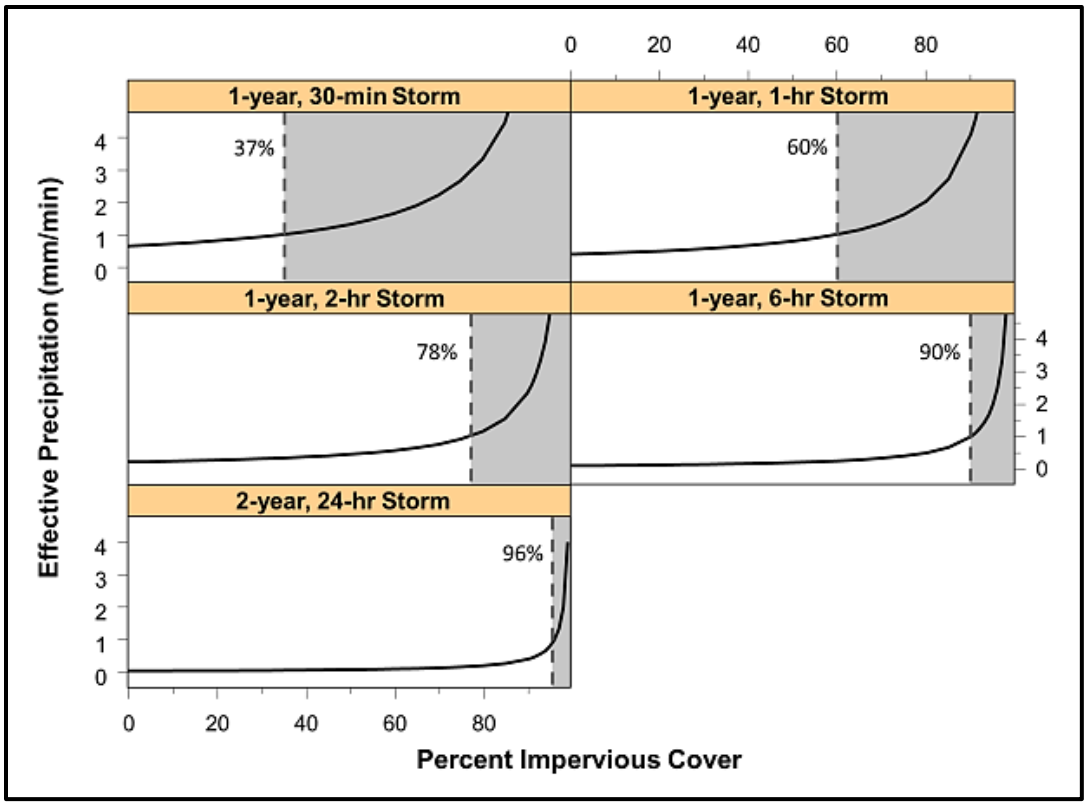

Figure 2.8: Effective precipitation models. The graphs show changes in effective precipitation for various storm events at increasing percentages of impervious cover. Greyed areas and dotted lines represent where the infiltration threshold of 1.05 mm/min was exceeded for each storm.

2.3.4 National Land Cover Data Analysis

The results from the GIS plot analysis were compared to coarser analyses, for example, data from the USGS National Land Cover Database (NLCD) (USGS, 2014) in order to assess the validity of using the NLCD data to determine areas with >60% impervious area. The imperviousness estimates of the two different methods were compared by averaging NLCD imperviousness measures within each of the thirty-eight plots and comparing the results to the measures found through the geospatial plot analysis.

In addition the distribution of plot analysis impervious cover was compared with impervious cover distributions for all of Allegheny County. This was done by finding the percent of regions that exceeded a certain percent impervious cover value for both methods and correlating the results (Table 2.3). The plot analysis correlated well with NLCD data for percent impervious cover values of 35-100%, but underestimates the number of regions with impervious cover values < 35%. Approximately 10.5% of the plots examined in the GIS impervious cover analysis had >60% impervious cover. This closely agrees with NLCD data which approximates that 10.6% of regions within Allegheny County are covered by >60% impervious cover (Table 2.3). According to the NLCD, areas containing >60% impervious cover typically lie along the river edges and within the city of Pittsburgh (Figure 2.9). Approximately 35% of the areas within the City of Pittsburgh contain >60% impervious cover.

Table 2.3: Distribution comparisons. The table below displays cumulative distribution of impervious cover as found by the Plot Analysis and National Land Cover Data.

	National Land Cover Data		Plot Analysis	
X % Impervious Cover	Number of 900m^2 Areas with > X % Impervious Cover	Percent of 900m^2 Areas with > X % Impervious Cover	Number of 40,000m^2 Areas with > X % Impervious Cover	Percent of 40,000m^2 Areas with > X % Impervious Cover
95	29989	1.40 %	1	2.63 %
90	54016	2.52 %	2	5.26 %
85	76968	3.59 %	2	5.26 %
80	101140	4.72 %	3	7.89 %
75	127416	5.95 %	3	7.89 %
70	156689	7.32 %	3	7.89 %
65	189712	8.86 %	3	7.89 %
60	227187	10.61 %	4	10.53 %
55	269709	12.60 %	5	13.16 %
50	321096	15.00 %	5	13.16 %
45	380134	17.75 %	6	15.79 %
40	442128	20.65 %	8	21.05 %
35	502747	23.48 %	8	21.05 %
30	560527	26.18 %	12	31.58 %
25	618679	28.89 %	17	44.74 %
20	681540	31.83 %	22	57.89 %
15	749984	35.03 %	23	60.53 %
10	823656	38.47 %	29	76.32 %
5	926106	43.25 %	32	84.21 %
0	2141207	100.00 %	38	100.00 %

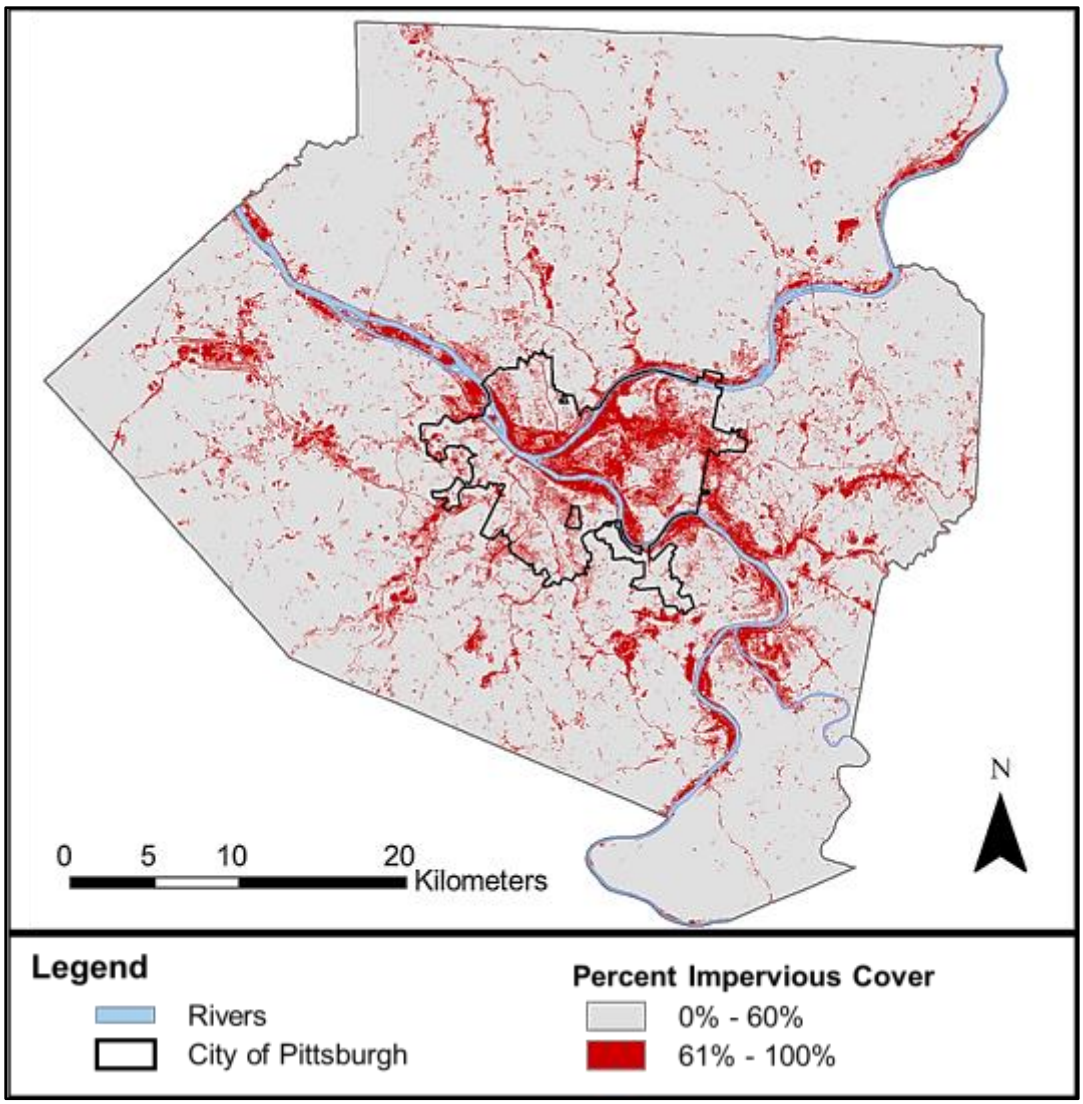

Figure 2.9: Regions in Allegheny County with >60% impervious cover. The geospatial data displayed is from the NLCD 2011 Percent Developed Imperviousness (USGS, 2014).

2.4 DISCUSSION

There is a limit to the infiltration of stormwater when effective precipitation (P_{eff}) rates from impervious cover exceed local soil infiltration capacities (see Section 1.4). In a case study of Allegheny County, PA, the P_{eff} rate of a 1-year 1-hour storm exceeded average infiltration capacities in regions with >60% percent impervious cover. Identifying site-specific thresholds could be useful in determining regions where high areas of impervious cover could contribute to decreased functionality of infiltration-based green infrastructure.

2.4.1 Infiltration Thresholds

In this study, a threshold-model was used to evaluate changes in P_{eff} rates at increasing areas of impervious cover and comparing these to averaged soil infiltration capacities across Allegheny County, PA. The average soil infiltration capacity of 1.05 mm/min was compiled from field measurements, local sources, and national databases, and was used as the threshold value. This was much greater than the median value of 0.55 mm/min because of the weight of a few high infiltration rate values, so this value may be conservative given the data That is, the average is an overestimate, with the pull of a relatively small percentage of high infiltration rates greatly skewing the mean. The higher values of infiltration capacity in the distribution were all from field measurements using the double-ring infiltrometer, and this method has been shown to yield higher values of infiltration if regions of preferential flow are created while driving the ring into the soil (Le Coustumer et al., 2009). It is also possible that the average value could be an underestimate, given most of the data below the average was from the Soil Survey national database. Soils are variable across landscapes and standardizing may not be representative of

individual catchments (Holman-Dodds et al., 2003). When evaluating the accuracy of using published values of surficial K_{sat} as proxies for true values of infiltration rates, Arrington (2013) found that values obtained from SSURGO data did not correlate well with measured data for that area due to coarseness of soil units. However, the study was very site specific and the database can still be more effective than other published datasets for large scale studies because of considerations to macropores and topography in K_{sat} calculations (Arrington et al., 2013).

2.4.2 Impervious Cover Analysis and Comparisons

In general, the plot analysis method of determining percent impervious cover was similar to NLCD estimates (Figure 2.10). The NLCD data did slightly underestimate regions with impervious cover >80%. This discrepancy is most likely due to the fact that coarse, data generated from remotely sensed reflectance cannot discern regions of impervious cover from pervious cover as effectively because of the uncertainties in unmixing reflectance. Therefore, the plot analysis method is a better predictor of impervious cover in densely urban areas than the NLCD.

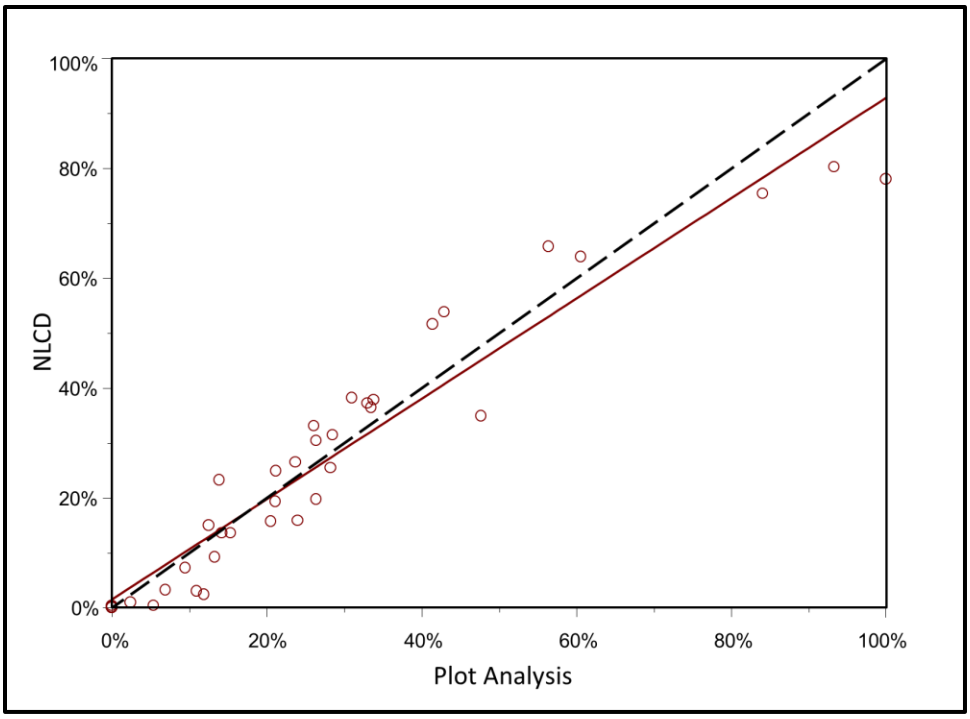

Figure 2.10: Impervious cover prediction comparison of NLCD vs. plot analysis. Red circles represent percent impervious cover for each of the thirty-eight GIS plots accompanied by a best-fit trendline (red). Black dotted-line represents a 1:1 correlation.

When considering impervious cover distributions, the imperviousness was used to classify regions as being urban, suburban, or rural. The EPA classifies urban areas (industrial, commercial and high-density residential) as regions with > 50% impervious cover, suburban areas (moderate-low density residential) as regions with 20-40% impervious cover, and rural areas with < 20% (EPA, 2011). The distribution of percent impervious cover generated from the plot analysis showed a majority of plots containing 0 – 40% impervious cover, which are considered rural or suburban, and only five contained >50% and are considered urban. The analysis did not yield the same distribution of percent impervious cover found by plotting NLCD (Figure 2.11), and this likely was due to a lack of representation of low suburban and rural areas in the transect plots. Distributions of high suburban regions and urban regions from the analysis

were similar to that found from NLCD. A larger, more distributed sampling of regions across the county would most likely lead to a more accurate representation of impervious cover distribution for future analyses.

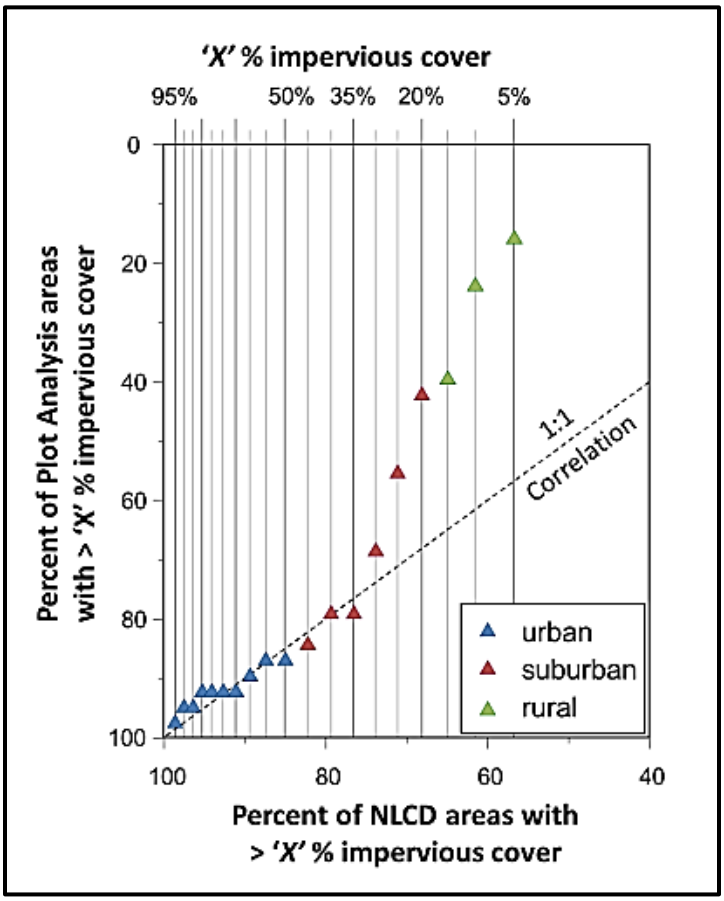

Figure 2.11: A correlation of percent impervious cover distribution of the plot analysis (y-axis) versus NLCD data (x-axis). Each point represents a value of percent impervious cover (ranging from 5%-95%), and the correlation compared the percent of regions from each analysis that contained greater than or equal to the given value of percent impervious cover. The proportion of suburban and rural areas was underestimated by the plot analysis.

2.4.3 Effective Precipitation and Implications for Green Infrastructure

The rainfall amounts obtained from point frequency data were converted into rainfall rates to make the values comparable to the average infiltration rate; if this value were exceeded it was assumed that that storm would produce runoff. Storms with shorter durations and longer reoccurrence intervals produced the highest rainfall rates (Table 2.1). Effective precipitation rates on pervious surfaces were calculated for each storm event with varying percent impervious cover. According to the model, increases in effective precipitation above base rainfall values are greatly enhanced in regions with >50% impervious cover (Figure 2.7), which are considered to be urban regions. Impervious cover threshold values varied by storm event, with smaller storms (higher initial rainfall rates) exceeding local infiltration rates at lower percentages of impervious cover (Figure 2.8). This means that, despite the fact that these storms produce lower volumes of total rainfall, the higher relative rainfall rates make P_{eff} more sensitive to increases in impervious cover.

Previous studies have shown the importance of modelling smaller, more-frequent storms in rainfall-runoff models in order to determine infiltration abilities of pervious areas (Damodaram et al., 2010; Holman-Dodds et al., 2003). An analysis of rainfall events in Pittsburgh shows that 95% of events are relatively small storms that produce 1 inch or less of total rainfall (Meliora, 2011), and because of this, most infiltration structures are designed to capture 1-inch of runoff (PADEP, 2006). Since a 1-year, 1-hour storm produces approximately 1 inch of rain and is a more frequent event, it was used as a standard around which to model local impervious cover thresholds, as opposed to the more commonly used 2-year, 24-hour storm. The 1-year, 1-hour storm exceeded local infiltration rates at an impervious cover threshold of 60%, which means that local soils would not be able to effectively infiltrate the volume of stormwater

generated in regions with greater than 60% impervious cover. However, only a small percent of regions within Allegheny County contain greater than 60% impervious cover, and these regions were predominantly located in the City of Pittsburgh and along the riverfronts. In fact, when analyzing distribution of percent impervious cover just within Pittsburgh, it was found that more than one-third of the city was covered by greater than 60% impervious cover. This can prove to be problematic for implementing infiltration-based green infrastructure in Pittsburgh; the city is a primary target for this type of stormwater management because its watersheds drain into CSO systems (ALCOSAN, 2008). This means that pervious surfaces for one-third of the city would be unsuitable for completely infiltrating the runoff load from adjacent pervious surfaces.

A few localized regulations suggest maximum loading ratios for the design of infiltration-based green infrastructure. This ratio is the measure of the maximum area of impervious surfaces that can drain into the infiltration area (PADEP, 2006). In Pennsylvania, a 5:1 maximum loading ratio is suggested, which equates to an infiltration system draining a region with 83% impervious cover. This is a standard used across the entire state, but may not reflect the requirements for individual watersheds. The maximum loading ratio should be adjusted to account for local limits to infiltration. The thresholds developed here can serve to adjust maximum loading ratios to more appropriate values for the site under evaluation. The standard ratio may be acceptable when designing the system to manage a 2-year, 24-hour storm, because rainfall rates would not exceed local infiltration rates until percent impervious cover equaled 96% (Figure 2.8). However, smaller, more frequent storm events with higher rainfall rates must be considered in the design, and using a 1-year, 1-hour storm would mean that maximum loading ratios for Allegheny County would have to be adjusted to no greater than 60% impervious. Other studies have noted the importance of adjusting conventional design standards in order to evaluate the sustainability

of infiltration-based green infrastructure within individual watersheds (Damodaram et al., 2010; Fletcher et al., 2013). Though these systems are best at capturing runoff from the smaller, more frequent storms (Brander et al., 2005; Holman-Dodds et al., 2003), these small storms have the potential of acting like larger storms due to effective precipitation from large areas of impervious cover in densely urbanized regions. For Pittsburgh, this would mean that infiltration systems may not be effective in areas with greater than 60% impervious cover.

Treating high percent impervious cover regions with infiltration systems is effective for run-off reduction to sewers and streams because these regions generate the largest volumes of surface runoff (Perez-Pedini et al., 2005). This is best done in regions with high infiltration rate soils and with many distributed systems throughout the catchment (Brander et al., 2005; Williams and Wise, 2006), but infiltration systems in urban Pittsburgh will be more isolated due to lack of available space and will be built in lower infiltration rate soils. These structures are designed to capture and store the first 1 inch of precipitation from all adjoining surfaces by increasing the structure dimensions (Gilroy and McCuen, 2009); however, by connecting any infiltration-based green infrastructure to large areas of impervious cover, it would act like a soil pipe conveying large concentrations of pollutants directly into the subsurface (Figure 2.12). The concentration of pollutants being carried in stormwater increases with increasing total impervious cover (Arnold and Gibbons, 1996; Glick, 2009), so infiltration systems installed in densely urbanized areas would experience rapid degradation through decreased permeability due to clogging through (Dechesne et al., 2005; Pitt et al., 1999; Reddi et al., 2000). When the risk of clogging is high or the hydraulic conductivity of the surrounding soils is low, designers can over compensate by artificially increasing conductivity within the systems. However, this has been shown to ultimately enhance clogging rates (Le Coustumer et al., 2009) and decrease filtration effects,

allowing contaminants to escape into local soils and groundwater reservoirs (Mikkelsen et al., 1996; Weiss et al., 2008). Infiltration systems installed in areas of Pittsburgh with >60% impervious cover run the risk of being rapidly degraded from sediment inputs and conveying contaminants to local groundwater reservoirs.

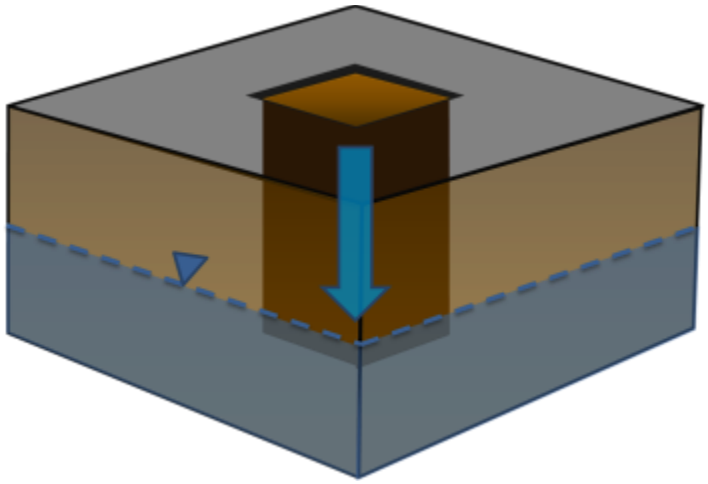

Figure 2.12: Stormwater soil pipe. In filtration systems in regions with high percent impervious cover can convey large volumes of contaminated stormwater directly to groundwater.

Despite limitations to infiltration-based infrastructure in densely urbanized areas, the benefits of runoff reduction cannot be ignored, and preliminary, site specific analyses must be made first to decide the best approach to minimize risks of structural failure (Barbosa et al., 2012). Infiltration systems can be distributed throughout suburban catchments where percent impervious cover is lower, but runoff still can have significant environmental impacts (Loperfido et al., 2014). Though densely urbanized areas of Pittsburgh have significant runoff production and contribute most to combined sewer overflow events (ALCOSAN, 2008), these structures might provide more challenges than benefits if installed within these regions. Infiltration systems can be augmented with other stormwater management practices in regions with high areas of

impervious cover to yield more sustainable results (Gilroy and McCuen, 2009). In fact, the best reduction of stormwater runoff came from using combinations of structures to detain and infiltrate stormwater from a wide range of storm events (Burns et al., 2012; Fletcher et al., 2013; Williams and Wise, 2006). The identification of impervious cover thresholds can be used to adjust design standards to better reflect local limits to infiltration, and can be used to help identify sections of urban areas that require augmentation of infiltration-based systems with additional stormwater management strategies.

3.0 STUDY 2: HILLSLOPE SOIL WATER DYNAMICS

3.1 BACKGROUND AND RESEARCH AIMS

Local organizations plan on installing infiltration-based green infrastructure in an urban park in Pittsburgh, PA, as part of the city's wet weather plan. The functionality of these structures will greatly depend on soil physical properties and subsurface soil water dynamics at the sites (Bouwer, 2002; Hamel et al., 2013), and each requires detailed site evaluations and modelling of local hydrological regimes before installation (Fletcher et al., 2013; Hamel et al., 2013). However, the tests commonly utilized for evaluation are spatially and temporally limited and may not give an accurate representation of site adequacy for infiltration-based green infrastructure (Bronstert and Bardossy, 1999; Göbel et al., 2004; Shuster et al., 2007). This study evaluates an alternative pre-monitoring technique that analyses the continuous, *in-situ* measurements of soil moisture to characterize hydrological regimes at the two sites in the urban park where infiltration-based green infrastructure will be installed. The objectives are to: (1) characterize subsurface soil water dynamics at the two sites (2) determine the implications for green infrastructure at these sites given the current hydrologic regimes, and (3) compare the efficacy of continuous spatial and temporal monitoring against more commonly used evaluation tools.

3.2 METHODS

3.2.1 Site Description

The study was conducted in south-western Pennsylvania in the Appalachian Plateau physiographic province. The local geology consists of nearly horizontal, repeated layers of interbedded of shale, siltstone, sandstone, and limestone (Wagner, 1970). The hills and valleys of the plateau region were generated by erosion from local streams and rivers, creating flat ridge-tops with steeply sloping valley walls that can be up to 100-150m tall (Wagner, 1970). Soils in this region are part of the Gilpin-Upshur-Atkins soil association according to NRCS Soil Surveys, and are characterized as being moderate- to very deep, well-drained colluvial silty-clay soils predominately derived from shale (Newbury et al., 1981).

Uplift and erosion of the landscape has caused horizontal and vertical stress-relief fracturing in both the valleys and hillsides in the Appalachian Plateau region (Figure 3.1). Groundwater flow along hillslopes is primarily downslope through subsurface soil processes and vertically into the bedrock through the fractures (Seaber et al., 1988). The vertical fractures along valley walls produce preferential flow paths for bedrock water downhill to the valleys (Seaber et al., 1988). Pressure from overlying rock layers causes fractures to close at greater depths in the valley, decreasing bedrock permeability and pushing water out into colluvial soils through springs or seeps in the hillsides (Harlow and LeCain, 1993). Springs and seeps can also develop from perched aquifers on the hillsides where impermeable soil or bedrock layers limit vertical flow (Kozar et al., 2012).

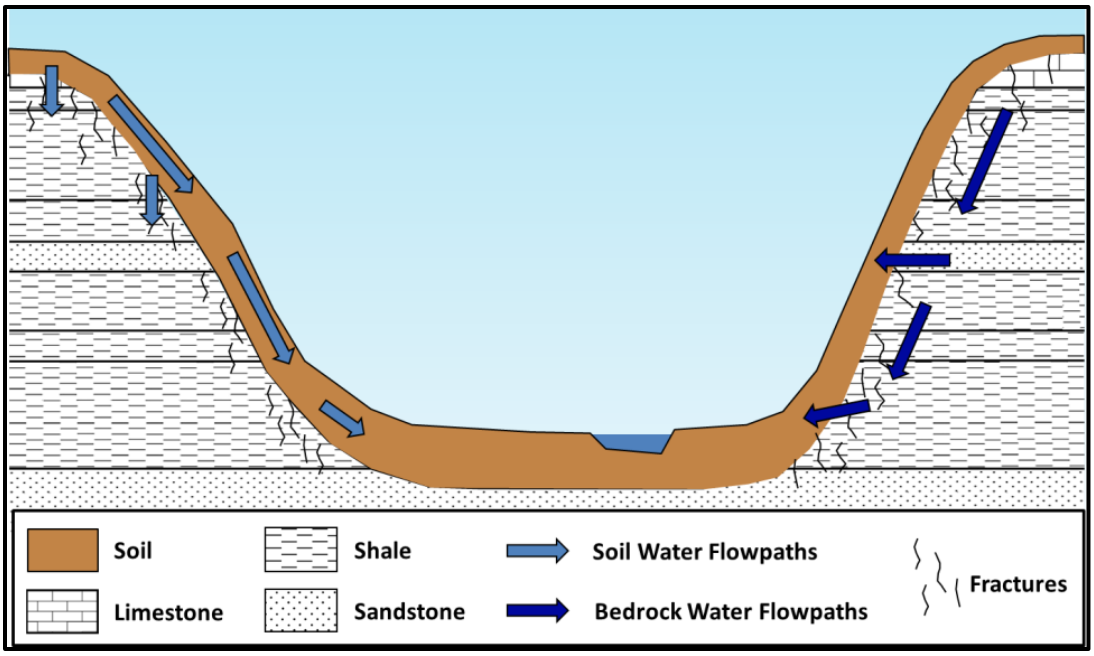

Figure 3.1: Bedrock and soil water flow along Appalachian Plateau hillslopes. Soil water flows laterally downslope and vertically into bedrock fractures. Bedrock water flows downslope through vertical fractures and out into colluvial soils when bedrock permeability is low. (Modified from Sheetz & Kozar, 2000).

The two study sites are located within Schenley Park in Pittsburgh, PA. The park is within the 4-Mile Run watershed, and contains the western half of the Panther Hollow subbasin (Figure 3.2). A majority of the streams in the watershed were redirected into the local combined sewer system during a phase of rapid urbanization in the watershed in the early 1900's (Hopkins et al., 2014). The combined sewer system, which is now more than one-hundred years old and beyond its design lifetime, accepts much of the catchment drainage and redirects flow into the Monongahela River (Hopkins et al., 2014). However, the portion of the subbasin within Schenley Park still drains into two above-ground streams, Phipps Run and Panther Hollow Run (Figure 3.3). As part of a watershed restoration project, infiltration-based green infrastructure is being installed at two locations within the park (Figure 3.2).

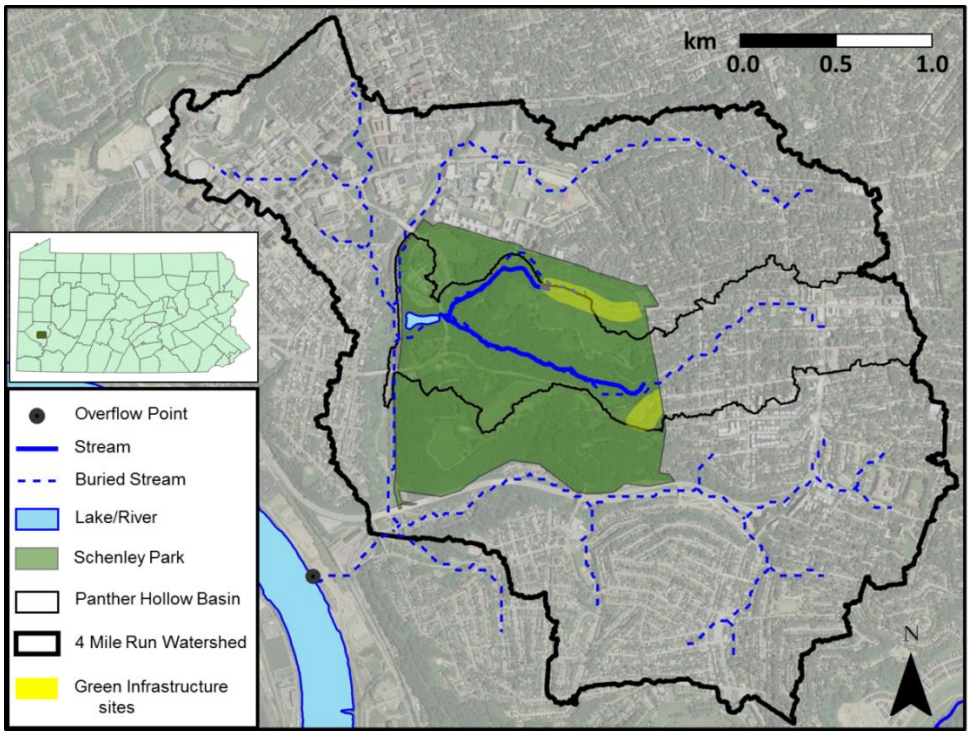

Figure 3.2: Schenley Park and the 4-Mile Run watershed. The urban park, located in Pittsburgh, PA contains the only two above-ground streams within the watershed. (Modified from Hopkins, 2014).

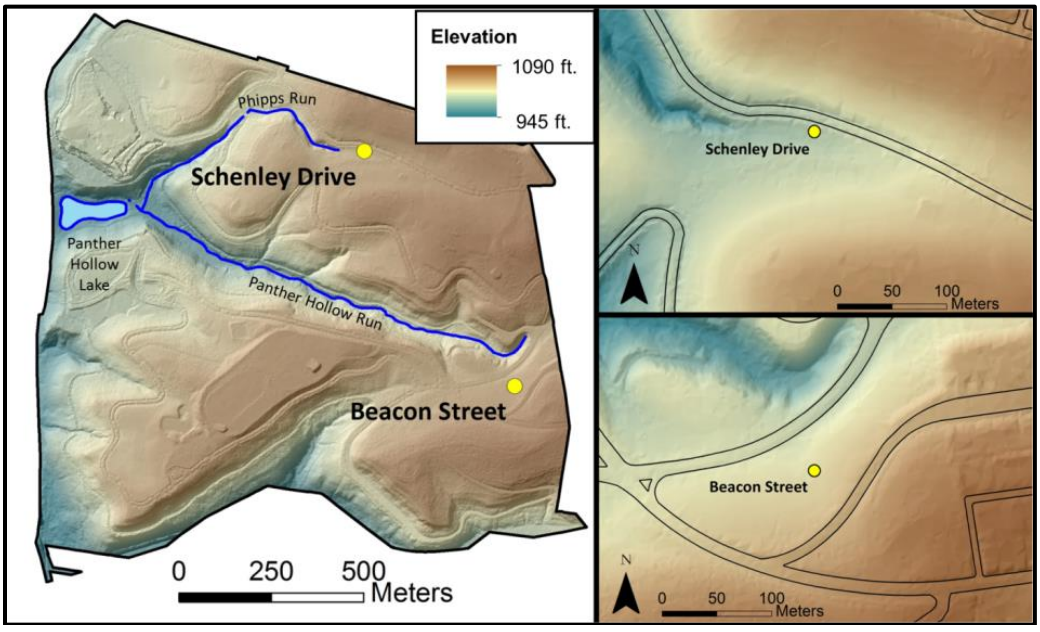

Figure 3.3: Digital elevation map of Schenley Park and the two study locations. Black lines represent road edges and yellow circles indicate the location of monitoring equipment.

Monitoring equipment was installed on hillslopes in these planned green infrastructure locations in 2012, and the sites were named Schenley Drive and Beacon Street, after the two nearest roadways (Figure 3.3). The hillslopes are both north-facing and covered by managed lawns. Soil pits were dug at each site for equipment installation, and the soil profiles were characterized using the NRCS soil texture classification system (NRCS, 1987). Soils were predominantly silty-clay (Figure 3.4) and contained subangular, gravel-sized clasts of shale regolith at depth.

3.2.2 Data Collection

Soil moisture was measured using HOBO® EC-5 Smart Sensors, model S-SMC-M005, and information from the probes was recorded using the HOBO® U-30 data logger. The sensors are dielectric probes that measure volumetric water content (θ_V) in m^3/m^3 with an accuracy of ±0.03 m^3/m^3. Dielectric probes are made of two parallel capacitance plates - one which sends out electrical pulses into the soil space between the plates, and the other which receives the pulse from the first plate. The change in frequency measured between the two plates can be directly attributed to the permittivity, or dielectric constant, of the soil (Wobschall, 1978). The permittivity is a dimensionless measure of the dielectric properties of a substance created by molecular dipoles. The total permittivity of the soil is a sum of the permittivity of mineral grains, air, and water in the soil. Water creates a large dielectric constant of ~80 because of the large dipole created from the arrangement of the oxygen and hydrogen atoms in its molecule; therefore, it has a large influence on the total permittivity of the soil as opposed to air and minerals, which only display dielectric constants below five. Increasing water content causes the

total permittivity of the soil to increase markedly, and this increase can be detected by the sensors (Robinson et al., 2008).

Four sensors were installed at each site throughout the soil profile (Figure 3.4) before the installation of green infrastructure. At Beacon Street, the probes were installed at 11cm, 37cm, 64cm, and 83cm below the surface, while at Schenley Drive the probes were installed at 15cm, 40cm, 70cm, and 96cm below the surface. In this paper, these locations are referred to as "layers" in the soil, and are representative of sensor depth, not soil horizon. The layers at each site are referred to as the top, top middle, bottom middle, and bottom respectively (Figure 3.4). Data logging began on January 16, 2012 at Schenley Drive and on May 9, 2012 at Beacon Street. Water content measurements were taken at 1 minute or 5 minute intervals. Soil moisture data from the probes were recorded as volumetric water content (θ_V) in the data logger.

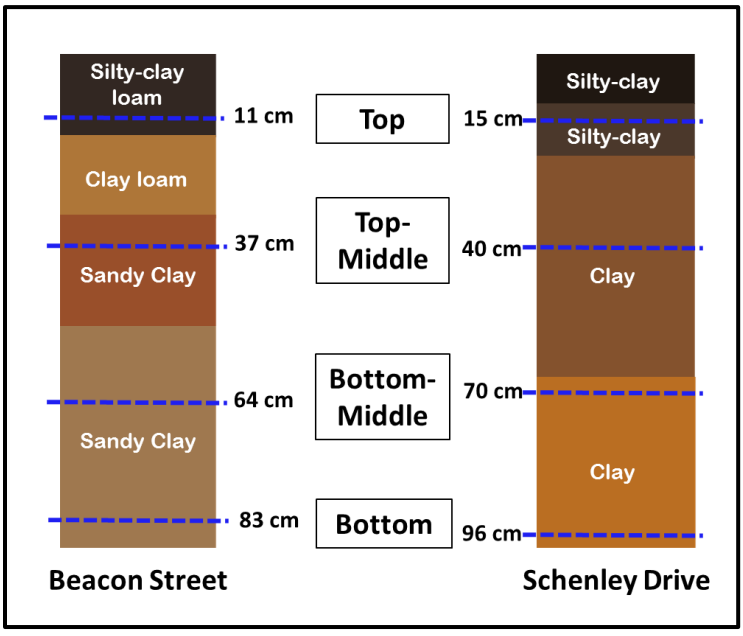

Figure 3.4: Soil profiles and sensor locations. Colors are approximate representations of the Munsell soil-color found in the profiles. Blue lines represent sensor locations.

3.2.3 Relative Saturation Calculations

The saturated water content (θ_{sat}) of the soils around each sensor was calculated through graphical and statistical analyses. Soil water responding to storm events plateaued at a point of saturation which was sustained over a span of time before draining again. These saturation plateaus can be observed as lower-amplitude peaks at the high-end tail of θ_V distributions curves (Figure 3.5).

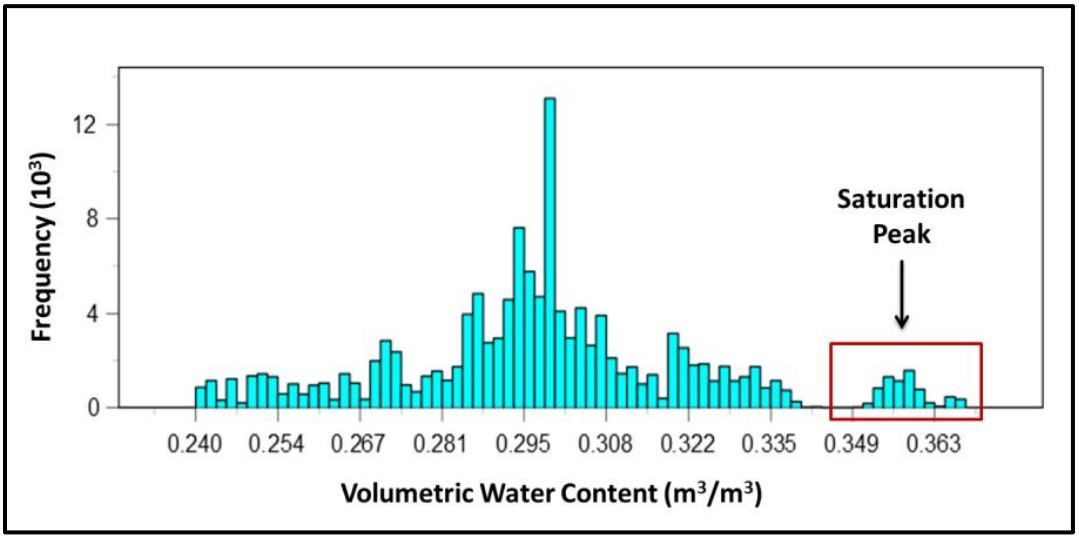

Figure 3.5: Saturation peaks as observed in volumetric water content distributions. The range of volumetric water content values contained within saturation peaks were used to estimate saturated water content for each soil layer.

Once these peaks were isolated, the average value was calculated and used as the saturated water content (θ_{sat}) for that soil layer. Relative saturation was calculated for each soil layer using its respective value of θ_{sat} and using the following equation:

$$\text{Relative Saturation (\%)} = (\theta_t/\theta_{sat}) \times 100$$

where θ_t is the volumetric water content (m^3/m^3) at time *t*, and θ_{sat} is the saturated volumetric water content (m^3/m^3). The resulting data were used to generate time series of relative saturation at each site. Soil moisture data were analyzed from May 1, 2012 to August 1, 2012, a pre-monitoring period before green infrastructure installation. This period was chosen for analysis as it was the only interval when all eight sensors recorded continuously without malfunction. The bottom sensor at Schenley Drive became impaired on July 27th, so subsequent dates were not included from the analysis for this soil layer.

3.2.4 Precipitation

Precipitation data were obtained from 3 Rivers Wet Weather, using their calibrated radar rainfall tool (3RWW, 2001). Rainfall measurements were obtained from the historical rain gauge data for the University of Pittsburgh station, located on the north-west border of Schenley Park. Rainfall totals were recorded at 15 minute intervals.

Storms were identified as being one distinct event if rainfall totals were consecutive and/or occurred within 120 minutes of the last recorded rainfall amount. Some storms that would normally have been characterized as one event were separated into distinct events if each pulse of rainfall caused an observable response in soil moisture in any particular soil layer (see July 4th example, Figure 3.6). Each individual storm event was analyzed for total rainfall and storm interval. The storm interval for a particular storm event was characterized as the time between the start of that storm and the end of the previous storm. Storm events with less than 0.06 inches of total rainfall did not cause responses in soil moisture for any of the layers and were not included in the analysis of storm response.

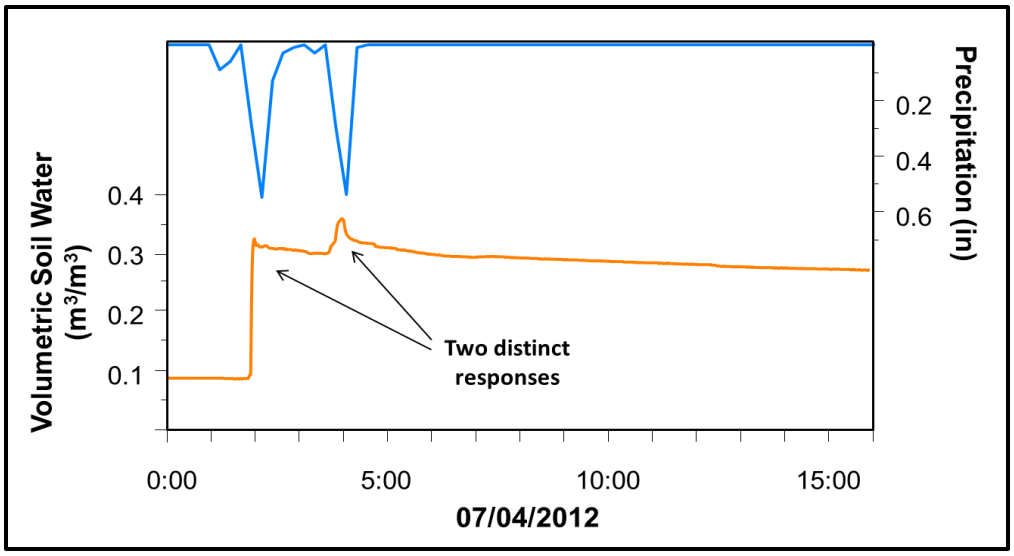

Figure 3.6: Distinct soil water responses to July 4th storm. This storm would typically be considered one event; however, since it caused two distinct responses in soil moisture, it was instead considered as two separate events.

3.2.5 Storm Response

A total of 38 storm events with rainfall totals above 0.06 inches occurred from May 1, 2012 to Aug 1, 2012. Time series of soil moisture and precipitation revealed observable soil water responses to storm events (Figure 3.7). To analyze each response, the antecedent soil moisture conditions were determined for each soil layer immediately preceding a storm event (Figure 3.7[A]). If the soil layer displayed an observable response, it was analyzed for lag time, peak soil moisture value, and saturation peak duration. The lag time is characterized as the amount of time it takes for the soil layer to reach peak soil moisture after the start of the storm event (Figure 3.7[B]), and saturated peak duration is the amount of time soils retain stormwater before being gravity drained back to field capacity (Figure 3.7[C]). Field capacity was assumed qualitatively as the steady-state reached immediately after stormwater drainage (Figure 3.7[D]).

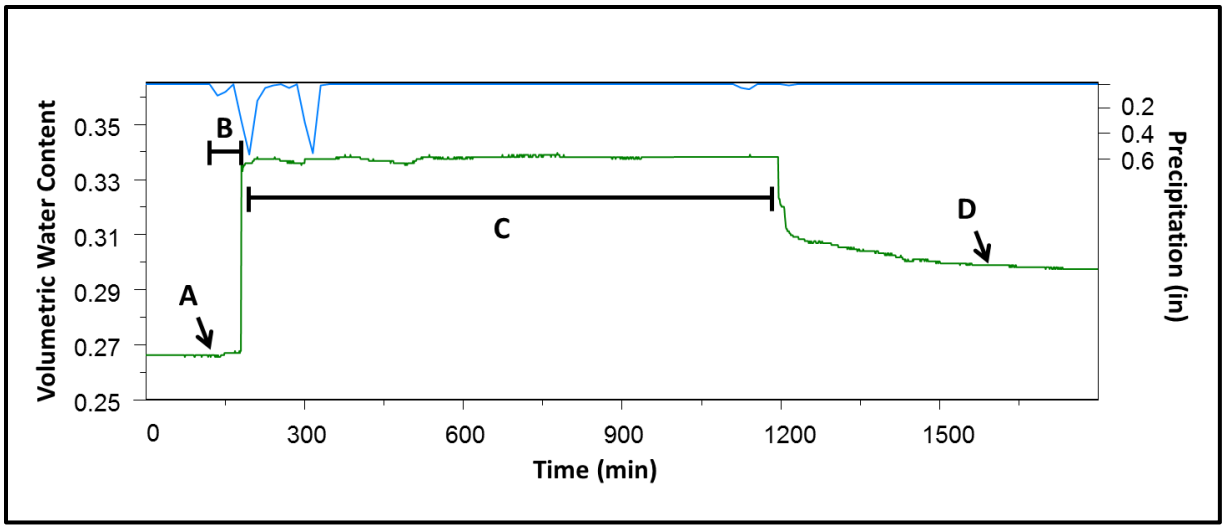

Figure 3.7: A representative soil moisture storm response. Storm responses were analyzed for **[A]** antecedent soil moisture conditions, **[B]** lag time, **[C]** saturation peak duration, and **[D]** field capacity.

3.3 RESULTS

3.3.1 Relative Saturation Analysis

To calculate the relative saturation of the soils over time, histograms of volumetric water content (θ_V) during the period of analysis were generated for each sensor location. Once the saturation peak was isolated, the average value was taken as the saturated water content (θ_{Sat}) for that particular soil layer (Table 3.1). At Beacon Street, θ_{Sat} values ranged from 0.344 m^3/m^3 in the top-middle layer to 0.357 m^3/m^3 in the bottom middle layer, and at Schenley Drive, θ_{Sat} values ranged from 0.330 m^3/m^3 in the bottom layer to 0.356 m^3/m^3 on the top layer. The saturation peak distributions were within the accuracy of the sensors.

Table 3.1: Saturated water content analysis results for Beacon and Schenley. The table displays the minimum, maximum, and average θ_V of saturation peaks in soil moisture that was isolated from the data set for each individual soil layer.

Site	Soil Layer	Saturation Min (m^3/m^3)	Saturation Max (m^3/m^3)	Average Saturation (m^3/m^3)	Standard Deviation
Beacon Street	Top	0.350	0.369	0.352	0.001
	Top Middle	0.342	0.345	0.344	0.001
	Bottom Middle	0.350	0.369	0.357	0.004
	Bottom	0.346	0.354	0.350	0.002
Schenley Drive	Top	0.346	0.369	0.356	0.005
	Top Middle	0.345	0.368	0.354	0.004
	Bottom Middle	0.350	0.369	0.346	0.005
	Bottom	0.328	0.341	0.330	0.003

Once θ_{Sat} values were determined, continuous records of relative saturation were generated for each soil layer at both sites for May 1st – August 1st, 2012, with records at Beacon Street beginning May 9th (Figures 3.8 & 3.9). The top layers had the lowest average relative saturation and the largest temporal variation in relative saturation (highest standard deviation) over time when compared to deeper layers across both sites, though Beacon had a lower average than Schenley (Beacon, 66.9 ± 17.8%; Schenley, 76.0 ± 16.3%) (Table 3.2). The top-middle layers had similar average relative saturation but differed in variation (Beacon, 88.7 ± 10.2%; Schenley, 84.2 ± 7.1%). The bottom-middle layer at Beacon had a similar average value to its top-middle layer, but varied less (84.0 ± 5.8%). However, the bottom-middle layer at Schenley had a much lower average value than its top-middle layer, though it had equally low variation (77.7 ± 7.7%). Beacon's bottom layer had the highest average relative saturation value of all the soil layers across both sites and the second lowest variation (93.0 ± 5.8%), whereas Schenley's bottom layer had an average value similar to its top-middle layer but varied the least (83.4 ± 4.5%).

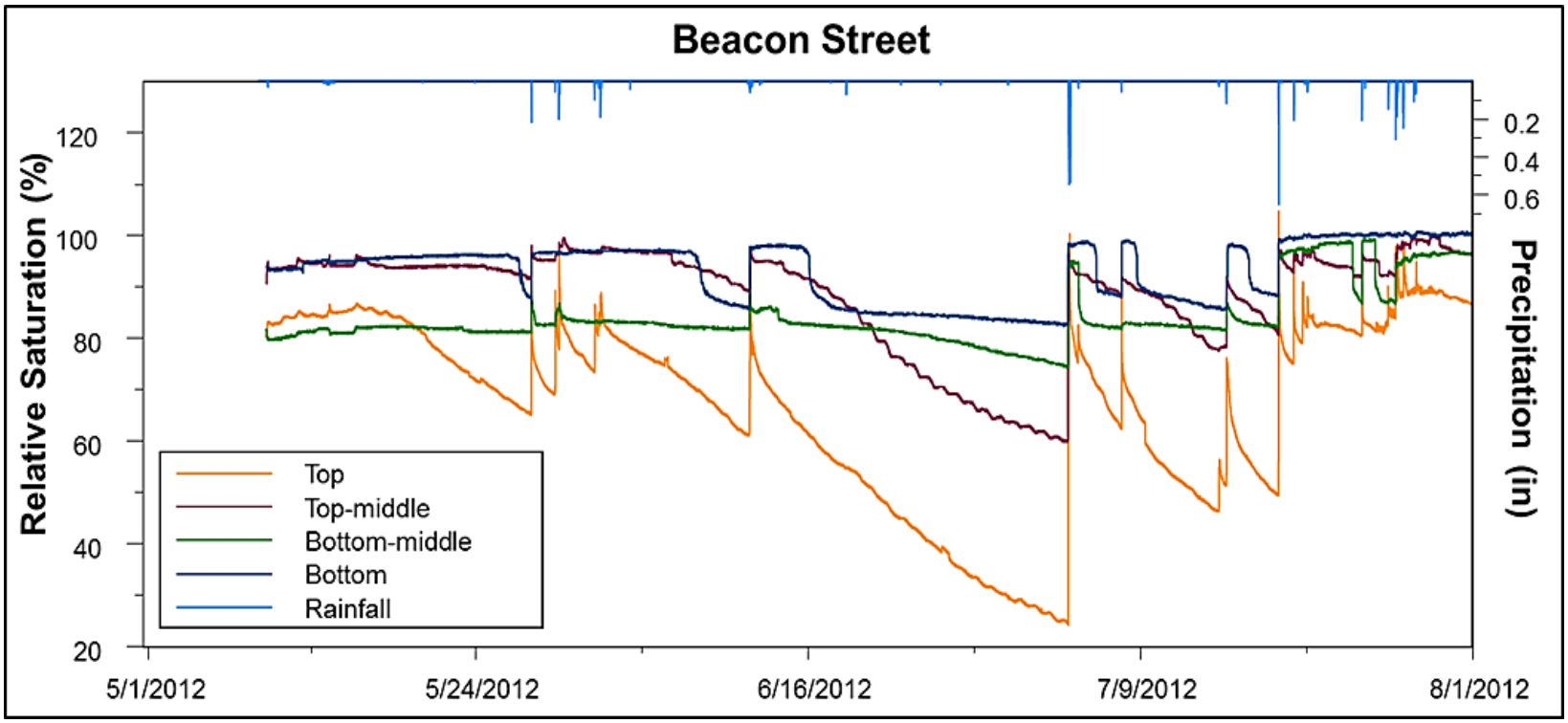

Figure 3.8: Continuous records of relative saturation at Beacon Street. The plot shows precipitation (light blue) and soil relative saturation for the top (yellow), top-middle (red), bottom-middle (green), and bottom (dark blue) layers at Beacon Street from May 9th to August 1st (2012).

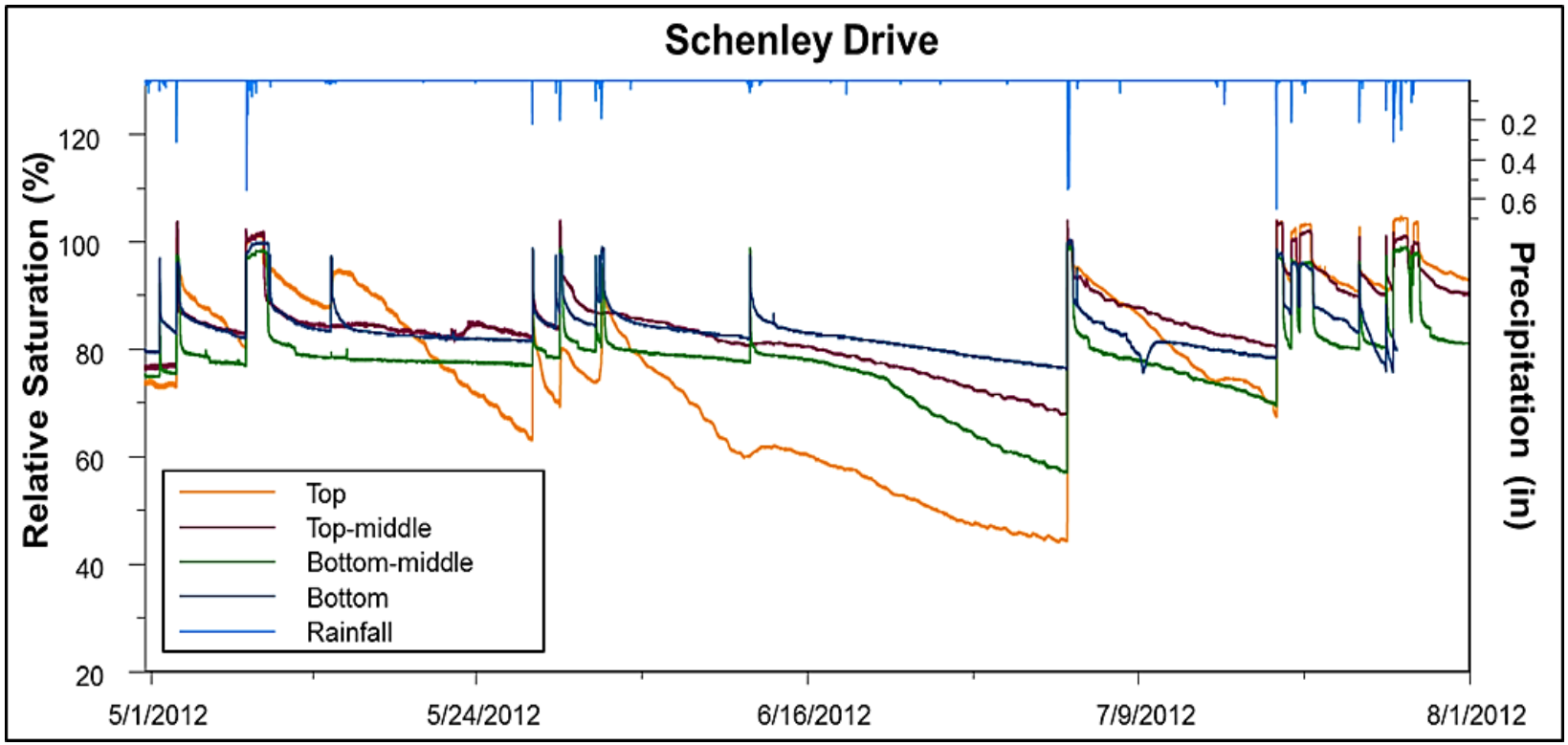

Figure 3.9: Continuous records of relative saturation at Schenley Drive. The plot shows precipitation (light blue) and soil relative saturation for the top (yellow), top-middle (red), bottom-middle (green), and bottom (dark blue) layers at Schenley Drive from May 1st to August 1st (2012). Data after July 26th was removed from the bottom layer due to sensor malfunction.

Table 3.2: Average and standard deviation of relative saturation at the study sites.

	Beacon Street				Schenley Drive			
	Top	Top Middle	Bottom Middle	Bottom	Top	Top Middle	Bottom Middle	Bottom
Average	66.9%	88.7%	84.0%	93.0%	76.0%	84.2%	77.7%	83.4%
Standard Deviation	17.8%	10.2%	5.8%	5.8%	16.3%	7.1%	7.7%	4.5%

Relative saturation is shown for each sensor location (Figures 3.8 & 3.9) and displays patterns of soil wetting during storm events (spikes in relative saturation), saturation peaks (prolonged plateaus of high relative saturation), and drainage (declines in relative saturation). The top-middle, bottom-middle and bottom layers all remained relatively saturated at Beacon, averaging between 84.0-93.0% saturated and had small ranges of soil moisture values during the period of analysis. These same layers experienced a prolonged wet period from early May to mid-June as shown by the sustained peaks in saturation (Figure 3.8). The top layer also experienced this prolonged saturation briefly until mid-May. Then, from mid-June to mid-July, relative saturation declined for all of the layers except the bottom, suggesting this was a relatively dry period. Subsequently, a series of frequent storm events after mid-July caused all of the soil layers to have prolonged saturation peaks. The top-middle and bottom layers displayed the highest sustained relative saturation during wet periods. During the dry period, relative saturation declined the most in the top and top-middle layers. For the entire period of analysis, the bottom layer had the longest sustained peaks and the highest relative saturation.

Though Schenley experienced the same wet-dry-wet pattern as Beacon, saturation peaks were not as prolonged and distinct patterns in relative saturation were not observable between the different periods (Figure 3.9). Instead, wet periods were marked by increased frequency of saturation peaks, but relative saturation declined more rapidly to field capacity after peaking. The

soil layers at Schenley displayed mean relative saturations which were typically 10% lower on average than Beacon soils, except those in the top layer. Overall, Schenley had shorter saturation peaks and steeper declines in relative saturation in its top-middle, bottom-middle, and bottom layers when compared to those at Beacon.

3.3.2 Precipitation Analysis

Precipitation data were obtained from the 3 Rivers Wet Weather calibrated radar rainfall data for the University of Pittsburgh rain gauge (3RWW, 2001). Storm events with total rainfall amounts ≥ 0.06 inches were identified and analyzed for rainfall totals and storm intervals (Table 3.3). There were a total of 38 storm events from May 1st to August 1st amounting to 11.32 inches of precipitation. Ten of the storms occurred before monitoring began at Beacon Street on May 9th. June was the driest month, with the least number of storm events (8 total) and the smallest average storm size (0.16 in.), whereas July was the wettest month with the highest number of storm events (17 total) and the highest average storm size (0.38 in.). The longest storm interval was between June 18th and July 4th and caused a fifteen-day dry period. The largest storm occurred on July 4th and had a rainfall total of 2.04 inches. However, in the analysis this large storm was considered as two separate events (07/04/2012 1:15, 1.16 in. and 07/04/2012 3:30, 0.88 in.) despite occurring less than two hours apart (see Figure 3.7). This is because the second portion of the storm caused observable storm responses in soil layers that were distinct from the responses to the first portion. A storm on July 27th was separated into two separate events for similar reasons (07/27/2012 4:45, 0.19 in.; and 07/27/2012 6:00, 0.31 in.). The second largest storm event also occurred in July (07/18/2012, 1.32 in.). The greatest addition to rainfall totals occurred in early May and mid-late July (Figure 3.10).

Table 3.3: Storm intervals and rainfall totals for storms in May, June and July (2012). Sample size and average rainfall totals are display at the bottom.

Date/Time (MM/DD/YYYY hh:mm)	Rainfall Total (inches)	Storm Interval (hours)	Date/Time (MM/DD/YYYY hh:mm)	Rainfall Total (inches)	Storm Interval (hours)	Date/Time (MM/DD/YYYY hh:mm)	Rainfall Total (inches)	Storm Interval (hours)
May			**June**			**July**		
5/1/2012 2:00	0.08	178.3	6/1/2012 6:00	0.27	57.5	7/4/2012 1:15	1.16	368.4
5/1/2012 5:45	0.09	2.8	6/1/2012 13:00	0.07	4.8	7/4/2012 3:30	0.88	0.5
5/2/2012 0:00	0.12	17.8	6/1/2012 16:30	0.38	3.0	7/4/2012 17:45	0.07	13.3
5/2/2012 5:15	0.07	4.5	6/3/2012 17:30	0.06	47.5	7/7/2012 17:15	0.06	71.3
5/3/2012 4:15	0.43	21.0	6/11/2012 22:30	0.32	196.7	7/14/2012 10:30	0.11	161.3
5/8/2012 0:30	1.08	115.3	6/12/2012 3:45	0.07	2.5	7/14/2012 23:15	0.20	11.5
5/8/2012 2:30	0.17	1.3	6/12/2012 16:45	0.06	12.3	7/18/2012 13:30	1.32	85.2
5/8/2012 8:45	0.41	6.3	6/18/2012 16:45	0.07	140.5	7/19/2012 15:15	0.32	24.3
5/8/2012 16:30	0.11	5.8				7/20/2012 13:30	0.17	22.0
5/13/2012 15:15	0.26	115.3				7/24/2012 8:30	0.21	90.3
5/27/2012 21:45	0.23	332.2				7/26/2012 4:45	0.15	44.3
5/29/2012 13:00	0.14	39.0				7/26/2012 16:45	0.32	12.0
5/29/2012 19:30	0.43	5.0				7/26/2012 18:45	0.61	1.8
						7/27/2012 4:45	0.19	7.5
						7/27/2012 6:00	0.31	0.8
						7/27/2012 23:15	0.12	16.8
						7/28/2012 1:45	0.20	2.3
Count	13		**Count**	8		**Count**	17	
Average	0.28		**Average**	0.16		**Average**	0.38	
St. Dev.	0.26		**St. Dev.**	0.13		**St. Dev.**	0.37	

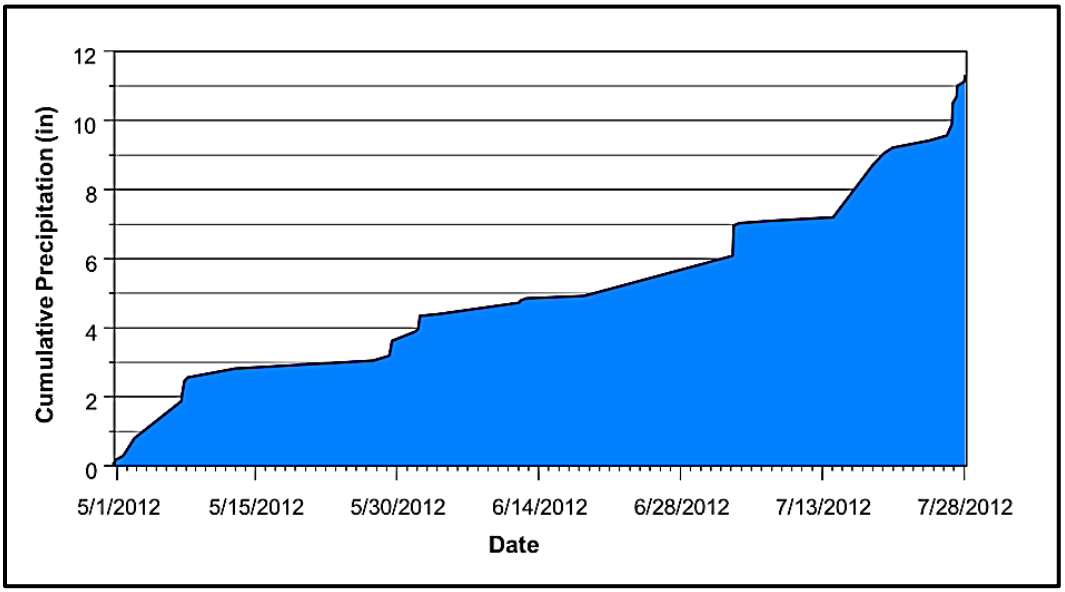

Figure 3.10: Cumulative precipitation plot for May 1st to August 1st (2012). Total rainfall over the period of analysis amounted to 11.32 inches.

3.3.3 Storm Response Analysis

The soil moisture time series were analyzed for storm response in each soil layer. A total of 38 storms occurred during May 1st – July 31st at Schenley Drive, and 28 storms occurred during the recorded time at Beacon Street (Figure 3.11). At Schenley Drive, the layers responded to 17, 14, 18, and 23 storms in the top, top-middle, bottom-middle, and bottom layers respectively. The bottom layers responded to the most number of storms, and, excluding the top layer, storm response increased with depth. At Beacon Street, the layers responded to 17, 13, 8, and 5 storms in the top, top-middle, bottom-middle, and bottom layers respectively. At this site, the top layer responded to the most number of storms, and the number of storm responses decreased with depth.

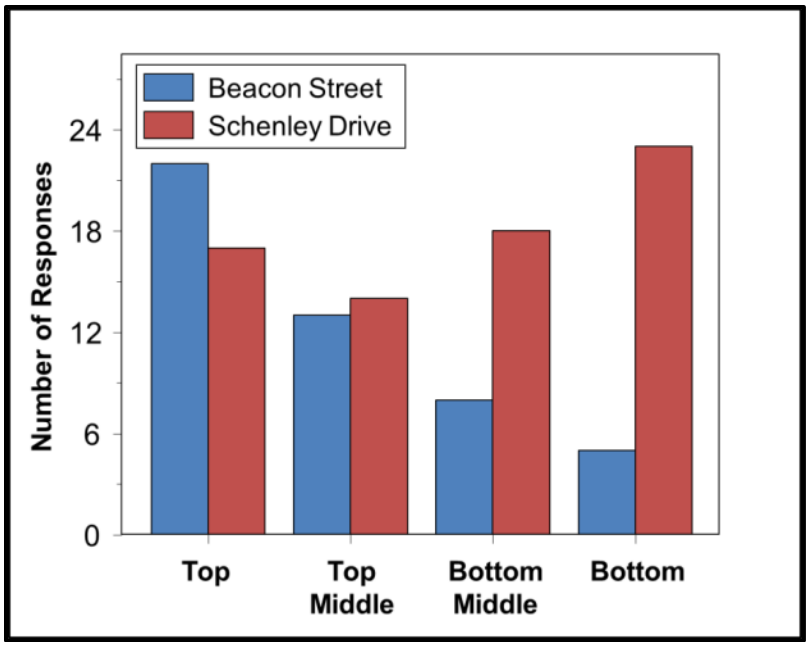

Figure 3.11: Frequency of storm response. The plot shows the number of storm responses in each soil layer at Beacon (blue) and Schenley (red).

The size of the storm and antecedent soil moisture conditions were analyzed to determine what factors would affect storm response at each site, using the Mood's median test for statistical analyses (Figure 3.12). At Schenley, antecedent soil moisture conditions did not have a significant effect on the response of soil water to storm events ($p>0.05$), but the storm magnitude significantly affected soil water response ($p<0.05$). However, storm size and antecedent soil moisture conditions both had significant effects on soil water storm response at Beacon ($p<0.05$). When analyzing response controls for each individual layer at Beacon, statistical tests showed that storm size had a significant effect on storm response for the top, top-middle, and bottom-middle layers ($p<0.05$), but storm responses in the bottom layer were significantly affected by antecedent soil moisture conditions ($p<0.05$) (Figure 3.13).

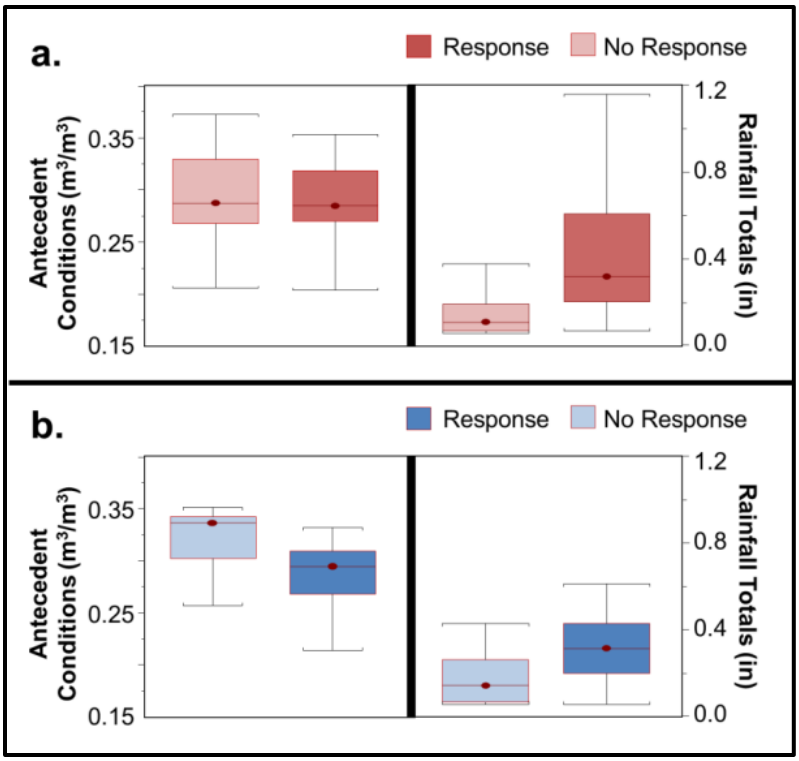

Figure 3.12: Storm response drivers at Beacon and Schenley. The box plots display average antecedent soil moisture conditions (m^3/m^3) and average rainfall totals (in.) for storm responses of all layers at **(a)** Schenley and **(b)** Beacon with outliers removed.

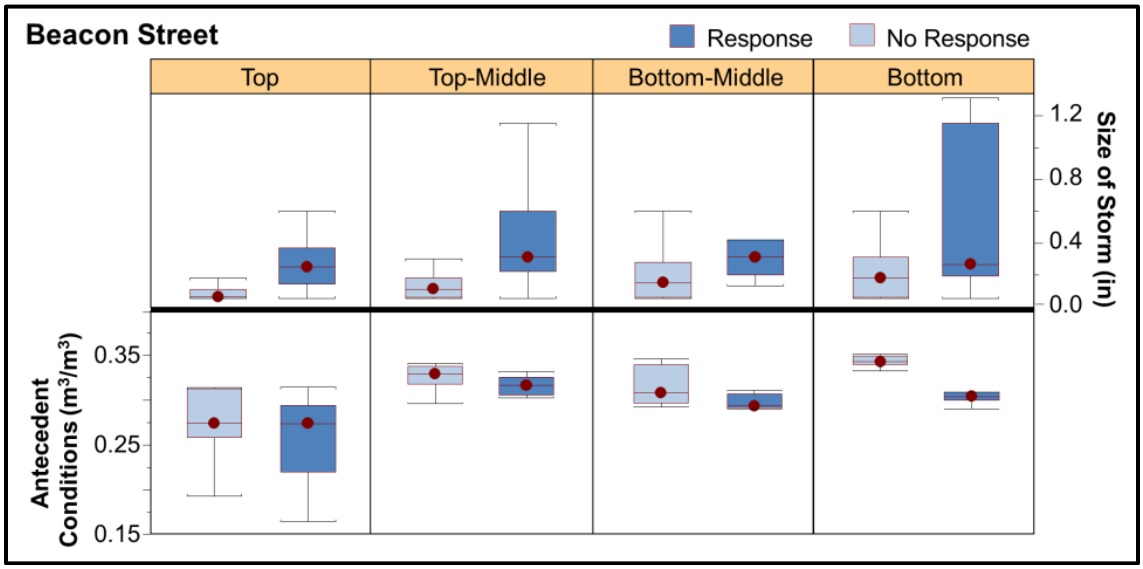

Figure 3.13: Storm responses drivers at Beacon, separated by soil layers. The box plots display average antecedent soil moisture conditions (m3/m3) and average rainfall totals (in.) for storm responses separated for each individual soil layer at Beacon with outliers removed.

Soil water responses in the soil layers were primarily driven by storm size for all layers at both sites except the bottom layer at Beacon. Each of these soil layers responded above a particular storm size threshold (Figure 3.14). At Schenley, the bottom layer and top layers had the lowest storm thresholds (0.07 in), and the middle layers had similar storm thresholds that were considerably higher than the other two (top-middle, 0.12 in; bottom-middle, 0.11 in). At Beacon, the top layer had the lowest storm threshold (0.06 in) and was similar to that of Schenley's top and bottom layers. A storm response to a 0.06 in. storm in the top-middle layer was considered an outlier, and thus the storm threshold was estimated at 0.20 in. The bottom middle layer's storm threshold was 0.14 in.

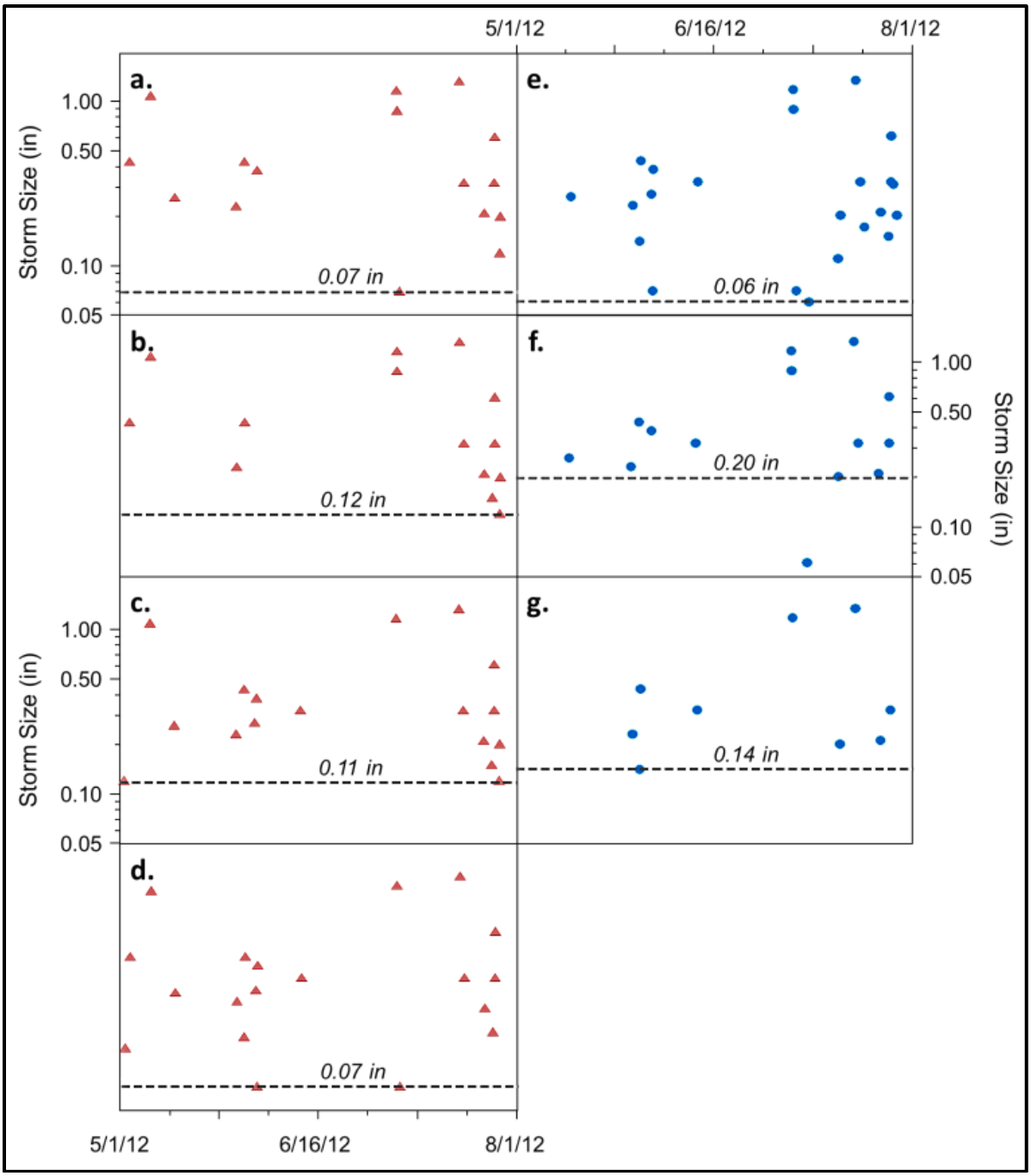

Figure 3.14: Storm thresholds for soil layers at Schenley (red) and Beacon (blue). Thresholds were estimated for layers in which storm size was the primary driver of storm response and are shown for Schenley **(a)** top, **(b)** top-middle, **(c)** bottom-middle, **(d)** bottom, and Beacon **(e)** top, **(f)** top-middle, and **(g)** bottom-middle layers. Beacon's bottom layer is not shown because its responses were not driven by storm size.

The order of wetting was analyzed at each site by comparing the times it took for each soil layer to respond (Figure 3.15). At Beacon Street, the top and top-middle layers (the upper layers) were the first to respond to a majority of storm events, but at Schenley Drive, the bottom and bottom-middle layers (the lower layers) were the first to respond to most storm events. Beacon Street only had two storm events where lower layers responded before upper layers (Storm 11, May 27th and Storm18, June 11th); for every other event, the lower layers responded after or at the same time as the upper layers. At Schenley Drive, the upper layers were consistently the last layers to respond, with the exception of Storm 23 (July 4th), the only storm where the top layer responded first.

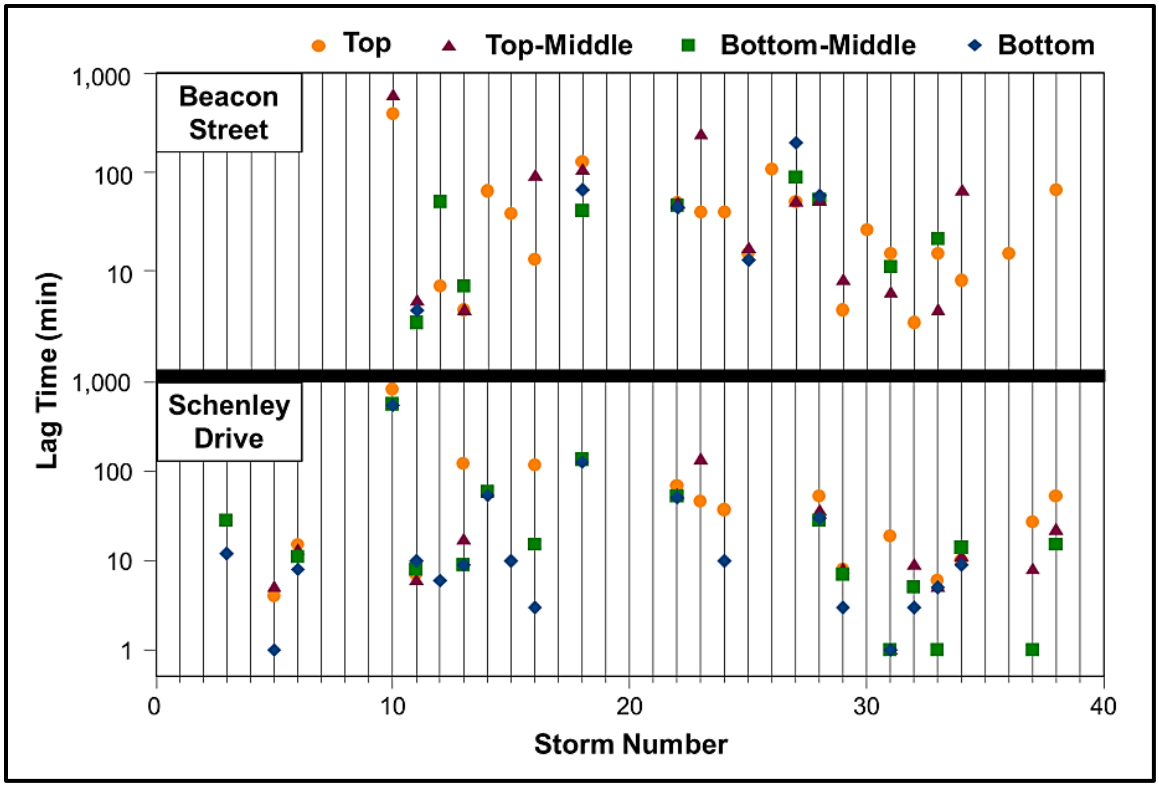

Figure 3.15: Storm response lag times. The plot shows the time (in minutes) it took for each soil layer to respond to storm events at the two sites. Storm number is sequential with the date of occurrence and equally spaced along the x-axis for better visual analysis.

3.3.4 Long- and Short-term Drainage Patterns

Long-term soil drainage patterns were analyzed by comparing antecedent soil moisture conditions and storm intervals (Figure 3.16). In general, longer storm intervals represent longer dry periods over which soil layers can drain, thus decreasing soil moisture levels. The rate of drainage was represented by the slope of the relationship between antecedent soil moisture conditions and storm interval, with steeper slopes indicating faster drainage rates. At Beacon, drainage rates decreased with increasing depth, with the highest drainage rates occurring in the top and the top-middle soil layers (-4.1×10^{-3} [m^3/m^3] hr^{-1} and -2.0×10^{-3} [m^3/m^3] hr^{-1} respectively). The bottom-middle and bottom soil layers had similar drainage rates (-1.4×10^{-3} [m^3/m^3]hr^{-1}, and -1.6×10^{-3} [m^3/m^3]hr^{-1}, respectively) which were relatively slower than those of the upper layers. The top layer at Schenley had the fastest drainage rate (-3.5×10^{-3} [m^3/m^3]hr^{-1}) relative to deeper layers at the site, and the bottom layer had the slowest drainage rate (-1.1×10^{-3} [m^3/m^3]hr^{-1}). The top middle (-1.8×10^{-3} [m^3/m^3]hr^{-1}) and bottom-middle (-2.3×10^{-3} [m^3/m^3]hr^{-1}) layers had slower drainage rates, comparable to the top-middle layer at Beacon. The soils at Beacon had higher antecedent soil moisture conditions than Schenley and relatively slower long-term drainage rates. The only exception is the top layer, which had both a higher drainage rate and lower antecedent soil moisture conditions than the top layer at Schenley.

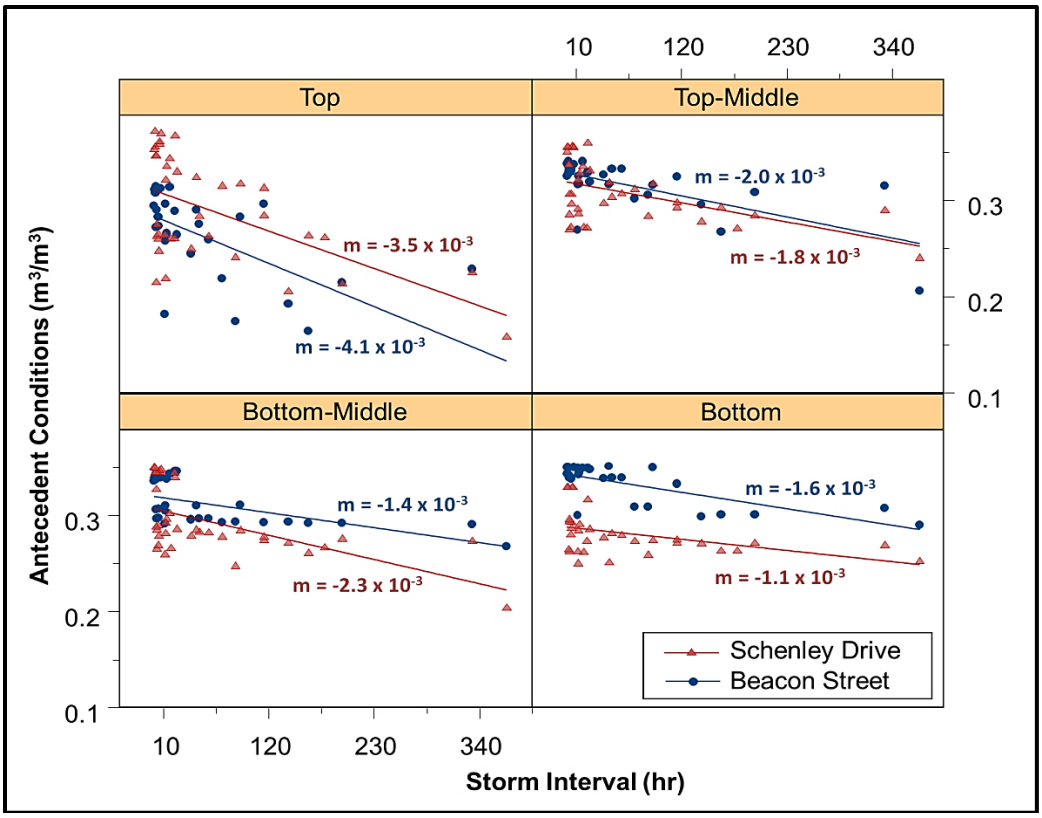

Figure 3.16: Long-term drainage rates. The plot shows antecedent soil moisture conditions (m^3/m^3) vs. storm interval (hr) for each soil layer at Beacon (blue) and Schenley (red). The relationship represents long-term drainage rates of soil water, with steeper slopes indicating higher drainage rates.

The top layer at Schenley appeared to have two distinct long-term drainage trends, which were isolated into an upper trend (higher soil moisture content) and a lower trend (lower soil moisture content) (Figure 3.17). The upper trend contained 21 storm events, and the lower trend contained 17 (Table 3.4). For the upper trend, 14 of the storms occurred in July, and the other 7 storms occurred in May, 4 of which occurred within the same day (May 8th). In the lower trend, only 3 of the 17 storms occurred in July, the others occurred in May and June. Conditions in the lower trend (May/June storms) had lower antecedent soil moisture conditions and slower drainage rates ($-2.6x10^{-3}$ $[m^3/m^3]hr^{-1}$), whereas the upper trend (July storms) had higher antecedent soil moisture conditions and faster drainage rates ($-4.4x10^{-3}$ $[m^3/m^3]hr^{-1}$).

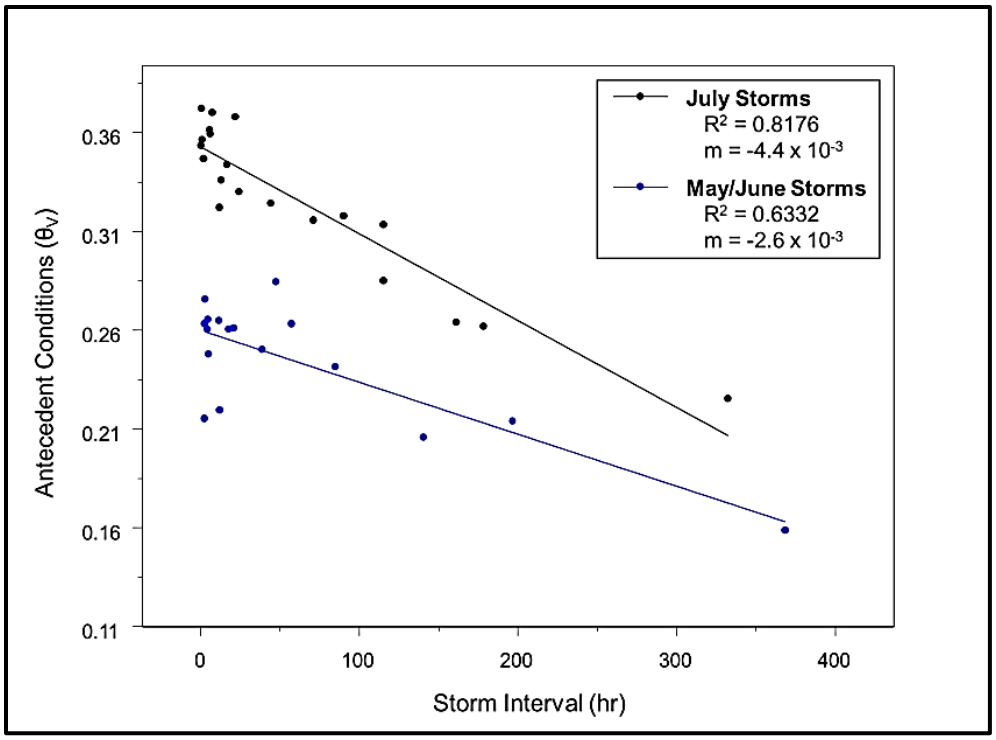

Figure 3.17: Seasonal trends at Schenley. Two distinct trends are observed in the top layer at when plotting antecedent soil moisture against storm interval. The upper trend (black) primarily contains July storms, whereas the lower trend (blue) is primarily contains May and June storms.

Table 3.4. Schenley storm events. Storms separated by date for the two trends in the top layer.

Upper Trend		Lower Trend		
May Storms	**July Storms**	**May Storms**	**June Storms**	**July Storms**
5/1/2012 2:00	7/4/2012 3:30	5/1/2012 5:45	6/1/2012 6:00	7/4/2012 1:15
5/8/2012 0:30	7/4/2012 17:45	5/2/2012 0:00	6/1/2012 13:00	7/14/2012 23:15
5/8/2012 2:30	7/7/2012 17:15	5/2/2012 5:15	6/1/2012 16:30	7/18/2012 13:30
5/8/2012 8:45	7/14/2012 10:30	5/3/2012 4:15	6/3/2012 17:30	
5/8/2012 16:30	7/19/2012 15:15	5/29/2012 13:00	6/11/2012 22:30	
5/13/2012 15:15	7/20/2012 13:30	5/29/2012 19:30	6/12/2012 3:45	
5/27/2012 21:45	7/24/2012 8:30		6/12/2012 16:45	
	7/26/2012 4:45		6/18/2012 16:45	
	7/26/2012 16:45			
	7/26/2012 18:45			
	7/27/2012 4:45			
	7/27/2012 6:00			
	7/27/2012 23:15			
	7/28/2012 1:45			

When soil water responded to a storm event, it reached a peak in soil moisture and sustained that peak for a period of time before being drained back to field capacity. The durations of these saturation peaks were used to characterize short-term drainage patterns for each soil layer after storm events (Figure 3.18). Beacon Street displayed a pattern of increasing peak duration with depth, but Schenley Drive had similar peak durations for all of its soil layers. In fact, Schenley Drive did not show any trends in peak duration, and average values did vary significantly between the soil layers ($p < 0.05$).

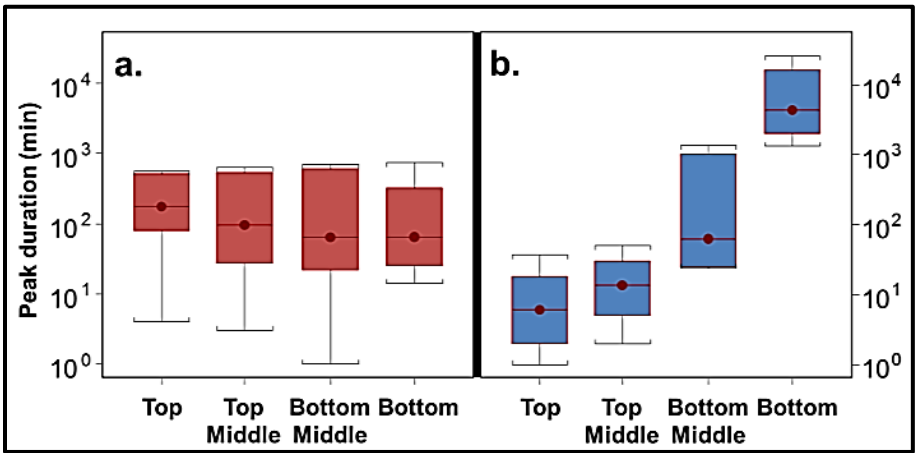

Figure 3.18: Average peak duration at Schenley **(a)** and Beacon **(b)**. Peak duration is assumed to represent short term drainage patterns for each soil layer.

3.4 DISCUSSION

The sites were found to have unexpected patterns in soil water dynamics which could lead to decreased hydrologic function of established infiltration-based green infrastructure. Traditional pre-installation evaluation tests likely are not able to detect the hydrological regime revealed by continuous monitoring.

3.4.1 Characterization of Hydrological Regimes

During the analysis period, soil water dynamics at the Schenley and Beacon sites (Figure 3.3) strongly contrasted. Average soil moisture at Beacon generally increased with depth, and as a result deeper soils remained fairly saturated. Variability in soil horizon characteristics can cause stratification of soil moisture during drier seasons (Penna et al., 2009). This was particularly noticeable at Beacon, where average relative saturation values were low in the top layer (66.9%) and much higher in the bottom layer (93.0%) (Table 3.2). In contrast, patterns of average soil moisture at Schenley were more inconsistent throughout the profile, but during the drier period, the deepest layer still remained more saturated than overlying soils. Generally, soils at Schenley were drier than those at Beacon and had a more restricted range of average relative saturation values (76.0-84.2%). The temporal variation of soil moisture in the top layer and bottom layer at both sites correlated with its average value, so that when soil layers had higher average soil moisture values they generally also had greater temporal variation of soil moisture values, and *vice versa* (Table 3.2). Other studies have found that soil moisture was less variable during wet

periods or within soil layers that remained predominantly saturated and more variable during drier seasons and in well-drained soils (Penna et al., 2009; Tromp-van Meerveld and McDonnell, 2006).

Long-term soil water drainage rates were analyzed at both sites by comparing antecedent soil moisture conditions with the storm interval. Drainage rates were highest within the top layers at both sites, and the layers experienced more complete drainage when compared to underlying layers. This can be attributed to evapotranspiration processes, which are highest during the dry, summer months. These processes, combined with vertical drainage of soil water into deeper layers, have been found to result in lower soil moisture values and rapid drying in near-surface soils (Mohanty et al., 2000; Western et al., 1999). Both sites are located on turfed landscapes, which have been found to have the most rapid drying rates in near-surface soils when compared to other forms of vegetated landcover (Qiu 2001). Slower drainage rates in underlying soil layers can be attributed to significantly lessened effects from evapotranspiration, because the shallow-root plants of turfed landscapes do not penetrate deep enough to dry deeper soil layers (Tromp-van Meerveld and McDonnell, 2006).

Long-term drainage patterns in the top layer at Schenley also revealed sub-seasonal trends in climate and evapotranspiration processes. In July, soils were typically wetter but dried more rapidly when compared to soil moisture conditions during May and June. A study from the Shale Hills Critical Zone Observatory, PA, with a similar climate, also found sub-seasonal trends in near-surface hillslope soils due to changing evapotranspiration rates from spring to summer (Takagi and Lin, 2012). The higher soil water content of the July trend is likely attributed to the larger, more frequent storm events that occurred in that month, and the more rapid drying is due to higher average daily temperatures and vegetation growth, which increases evapotranspiration

rates (Figure 3.19). Four storm events from May contributed to the July trend (see Table 3.4), but this was because all four storms occurred within one day, resulting in higher antecedent soil moisture conditions that were atypical for that month.

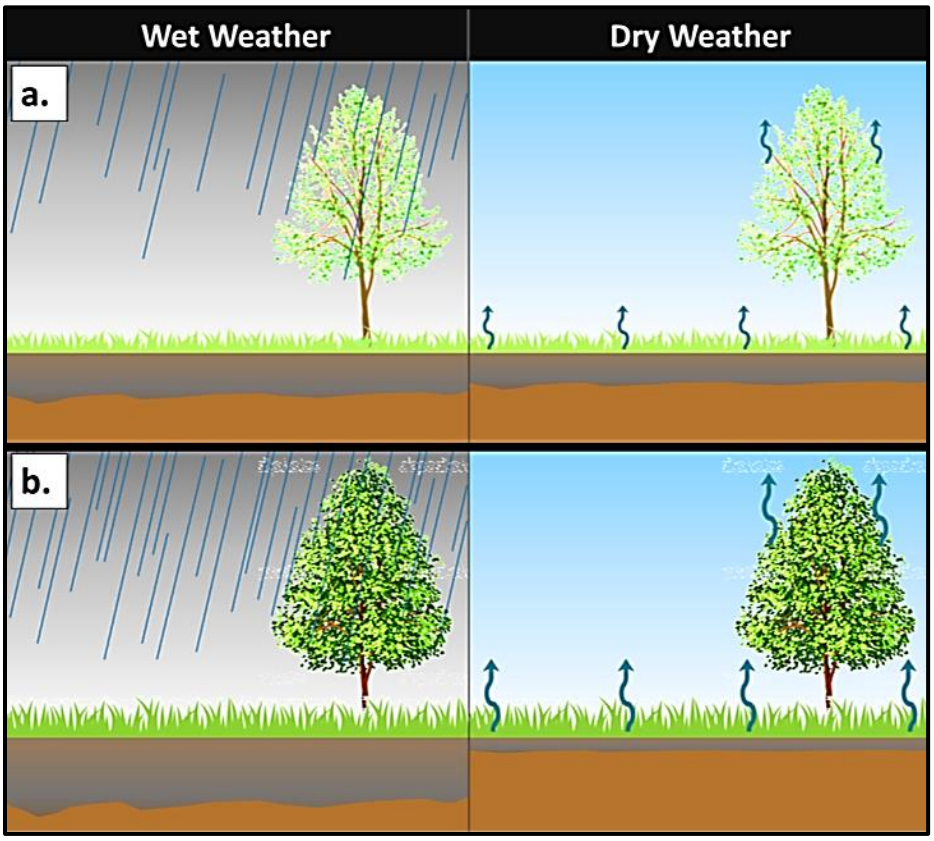

Figure 3.19: Sub-seasonal trends in evapotranspiration at Schenley. **(a)** In May and June, wet weather events were smaller and less frequent resulting in relatively lower water content in soils, and during dry weather evapotranspiration rates were lower (small blue arrows). **(b)** In July, wet weather events were larger and more frequent resulting in relatively high water content in soils, and during dry weather evapotranspiration rates were higher (large blue arrows).

In contrast to the top layers, long-term drainage rates of soil water in the bottom two layers at Beacon are considerably slower (Figure 3.16). This is likely attributed to low vertical fluxes in preferential flow, leading to prolonged periods of saturation. The high relative saturation and low long-term drainage rates of these two lower layers may be indicative of a

shallow groundwater table or a vertically extensive capillary-fringe zone above the bedrock. Long-term drainage rates at Schenley Drive were also very slow, but the soils were considerably drier than those at Beacon and are most likely not in contact with local groundwater tables during dry periods.

Short-term drainage rates were represented by analyzing soil moisture peak durations after storm events, which showed how long the layers retained stormwater before lateral and vertical fluxes drained soils to field capacity. Beacon had a sequential increase in peak duration with depth; that is, deeper soils retained water longer after storm events. The higher water retention correlates to lower long-term drainage rates, which is typical for deeper soils that receive vertically drained water from overlying layers (Hewlett and Hibbert, 1963). The soil layers at Schenley had close to uniform drainage throughout the soil profile after a storm event. The lower average soil water content and higher short-term drainage at Schenley means that the site is more completely drained throughout the soil profile as compared to Beacon.

Soil water responded to the frequency and magnitude of storm inputs throughout the entire depth of the soil profiles, but the patterns and number of responses varied between the two sites. At Beacon Street, the number of responses for each soil layer decreased with depth (Figure 3.11). When soil water in deeper soils did respond to storm events, the lag time was considerably longer than those in shallower soils (Figure 3.15). This hydrologic behavior suggests soils here experience top-down flow during wet weather (Grayson et al., 1997; Lin and Zhou, 2008), which occurs when a wetting front percolates vertically down through the soil profile from infiltrated stormwater at the soil surface (Figure 3.20). This is the natural wetting

regime for hilltops and hillslopes, which are considered to be areas of soil water recharge (Fetter, 2000; Bachmair and Weiler, 2011), and these patterns are particularly evident during dry summer seasons in temperate climates (Harr, 1977; Yeakley et al., 1998).

In contrast, soil water at Schenley displayed increased storm responses with depth, except in the top layer (Figure 3.11), and deeper soils consistently responded to storm events before shallow soils (Figure 3.15). The top layer at Schenley responded to a higher number of storm events than the top-middle layer, despite the general increasing trend with depth. In addition, the top layer responded to storm events first if lower layers were already too saturated to respond, as shown during the July 4th storm. These patterns suggest that stormwater was reaching the bottom layers first, and Schenley experienced a bottom-up wetting regime (Lin and Zhou, 2008) (Figure 3.20). The top layer soils still experienced top-down wetting; however, the downward vertical flow of stormwater was much slower than the upwards vertical flow of soil water from below. This wetting regime is more commonly associated with regions of discharge but is generally not assumed to occur along hillslopes (Fetter, 2000).

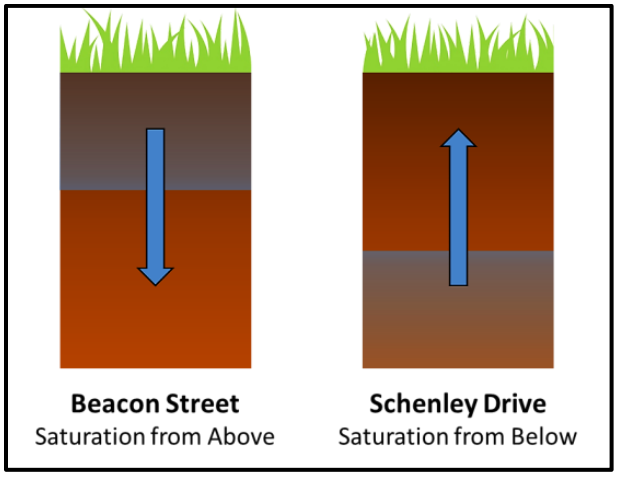

Figure 3.20: Preferential stormwater flow paths. Stormwater wetting fronts saturate soils at Beacon from the top to the bottom, but Schenley soils are saturated from the bottom layer up.

Some studies have found similar patterns in soil water dynamics like those found at Schenley and attributed it to water inputs from bedrock fracture flow at the soil-bedrock interface (Lin and Zhou, 2008; Montgomery et al., 1997). The flow of water through permeable bedrock layers has been recognized as an important component of local water balances, but most observations have shown the vertical movement of soil water into bedrock fractures to be predominant (Graham et al., 2010; Tromp-van Meerveld et al., 2007), especially in shale basins where little to no lateral movement is detected (Tsujimura et al., 1999). However, other studies have shown that the upwards response of soil saturation to storm events along hillslopes indicated that bedrock fracture flow contributed significantly to subsurface flow in shallow colluvial soils (Figure 3.21) (Anderson et al., 1997; Montgomery et al., 1997). Bedrock fracture flow was mostly prevalent in downslope regions, closer to streams, and much of the water was derived from recharge areas further upslope. However, decreased conductivity in relatively impermeable rock layers located higher up on the hillslope can force water out into the soils far above valley regions and can control hillslope runoff processes (Uchida et al., 2003). Bedrock fracture flow contributions to unsaturated soil flow were shown to be significant in a variety of geologic landscapes, including shale basins (Onda et al., 2001). It is therefore likely that subsurface lateral flow patterns at Schenley are also being driven by water inputs from bedrock fracture flow.

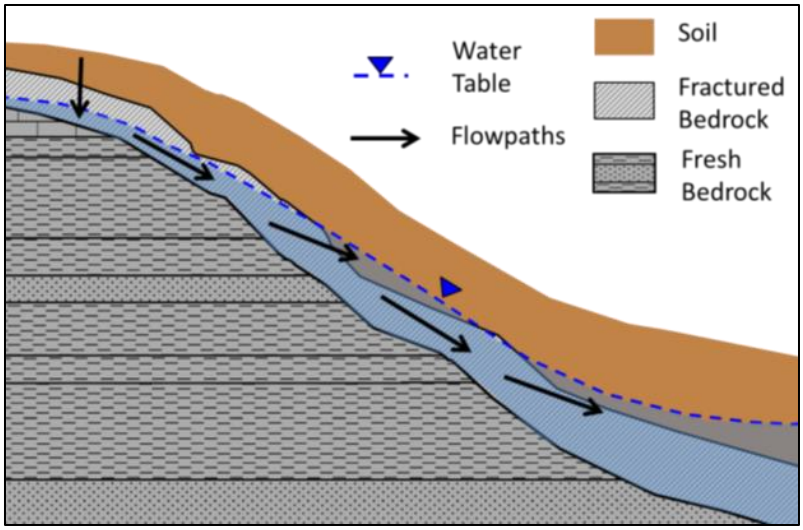

Figure 3.21: Bedrock fracture flow along hillslopes. Water from recharge areas along hilltops flow vertically into fractured bedrock and flows downslope, occasionally flowing out into overlying colluvium as springs or seeps. (Modified from Anderson 1997; not to scale).

Storm size and antecedent soil moisture conditions were found to be the largest drivers of storm response at Beacon and Schenley, which agrees with other studies of hillslope subsurface soil water dynamics (Penna et al., 2011; Tromp-van Meerveld and McDonnell, 2006). At Beacon, storm response was primarily controlled by the size of the storm in the first 64 cm of soil (top to the bottom-middle layer), though all layers were affected by antecedent soil moisture conditions to some extent. These layers would only respond to storms above a certain size threshold (Figure 3.14). Storm threshold values have been found in previous studies in unsaturated subsurface soils (Lin and Zhou, 2008; Tromp-van Meerveld and McDonnell, 2006). Soil water in the first 11 cm would respond to storm events larger than 0.06 in, whereas soil water in the middle layers typically did not respond to storm events smaller than 0.14 inches. During small storm events (< 0.14 inches), water inputs are not large enough to percolate downwards into the middle layers to cause a storm response. Soil water at depths of 83 cm (bottom layer) only responded to storm events if antecedent conditions were unsaturated. It is

possible that the water table lies at this depth or that it is within the capillary-fringe zone. For a water table to be sustained in hillslope soils like at Beacon, these soils would need to have particularly low hydraulic conductivity to inhibit groundwater drainage through downslope lateral flow (Penna et al., 2009). However, textural analyses show that deeper soils at Beacon contain sand and subangular gravel-sized clasts produced by weathering in the regolith, which should increase soil permeability and allow for sufficient lateral drainage of soil water. It is likely that the saturated conditions in deeper soils are sustained by water inputs from bedrock fracture flow. On a study of hillslopes in Japan, Uchida (2006) found that when bedrock-soil interfaces displayed sustained saturated conditions, it indicated that bedrock water storage was significant enough to flow upwards into colluvium even during baseflow. This could explain sustained saturated conditions at Beacon. The reason Beacon doesn't experience bottom-up wetting from the bedrock fracture flow like at Schenley could be a result of the sandier soils at depth allowing more rapid redistribution of water inputs downslope during storm events so that the water table does not rise rapidly into upper layers.

At Schenley Drive, storm response throughout the entire profile was primarily driven by storm size, because soils at Schenley Drive are able to drain more completely after storm events as compared to Beacon soils. The July 4th storm event is unique in that it gives us a better look at the hydrologic regime. On this date, two storms events occurred totaling 2.04 inches of rain within a three- hour period. These storms would typically be counted as one, however the second storm triggered soil water responses in the top and top-middle layers, but not the lower layers. This was the only time when the upper layers responded without one or more of the lower layers responding. Significant vertical drainage must have occurred in these two layers to allow for a second response, but not in the bottom soils, leaving them saturated and unable to respond again

to the second pulse of rainfall. This shows that a vertical wetting regime is only possible when the bottom layers are sufficiently saturated from a large storm event. This is the only time when Schenley storm response patterns mimicked those at Beacon.

Overall, Schenley soil water dynamics are driven by non-local controls from the sloping soil masses during dry periods, therefore draining downslope through both vertical and lateral pathways (Figure 3.22a). This results in more complete drainage of all soil layers and lower average soil moisture content as compared to Beacon. Evapotranspiration also contributes to high long-term drainage rates and lower average soil moisture contents within the top layer. During wet weather, bedrock fracture flow pushes stormwater up into overlying soils, leading to rapid bottom-up wetting regimes through the profile, but the top layer may still experience slower top-down wetting during large storms (Figure 3.22b). Soil water in upper layers of Beacon drain downslope through both vertical and lateral pathways during drain periods, resulting in lower average soil moisture contents, and more rapid short- and long-term drainage rates; however, the lower soil layers remained fairly saturated during dry periods and had slower short- and long term drainage rates, which was most likely attributed to bedrock water seepage into the overlying soils (Figure 3.22c). Just as at Schenley, high evapotranspiration rates in the top soil layer results in high long-term drainage rates and lower average soil moisture content. During wet weather, Beacon soils experienced top-down wetting regimes from downward vertical flow of stormwater, but soil water in lowers layers responded less to storm events due to high antecedent soil moisture conditions (Figure 3.22d).

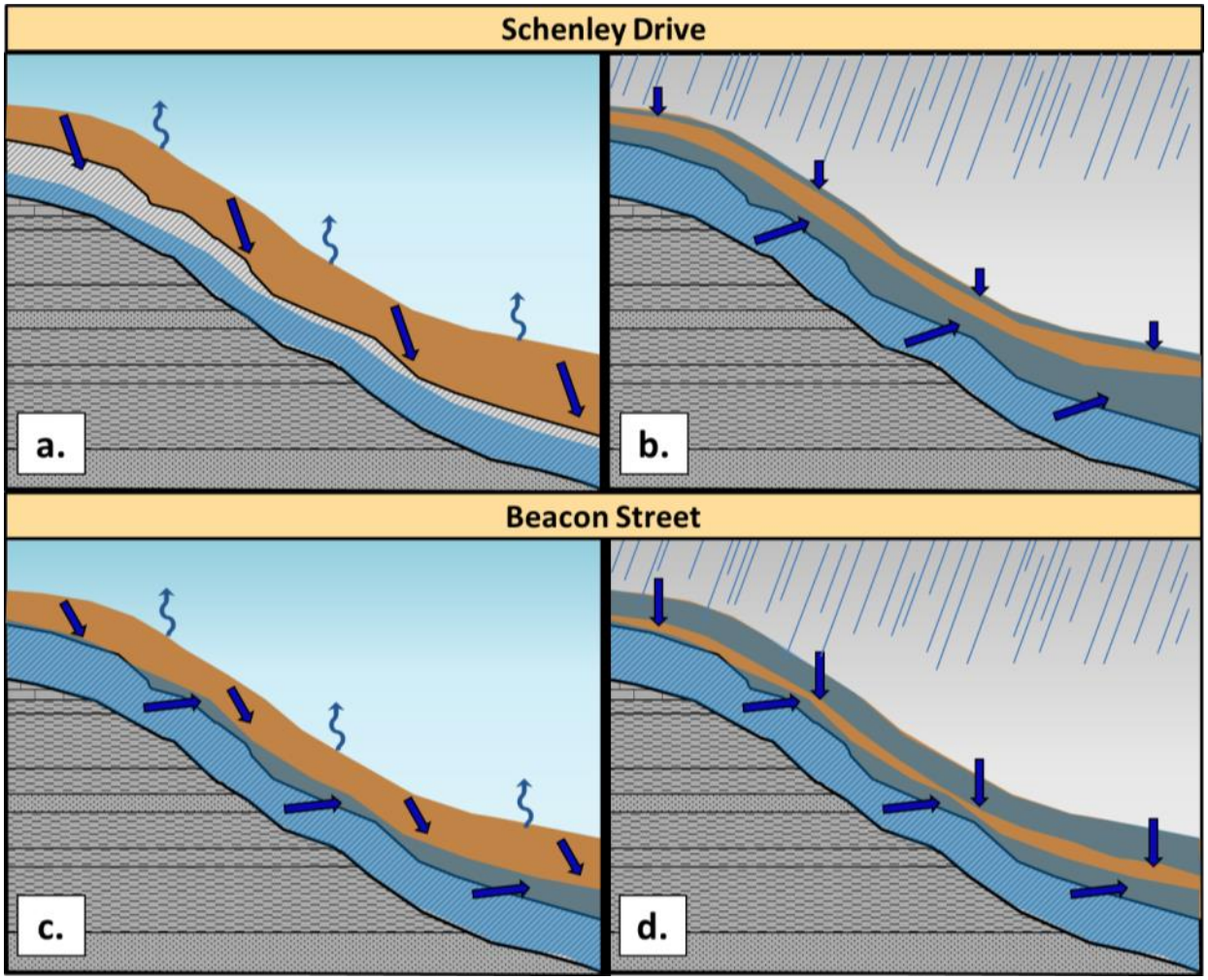

Figure 3.22: Subsurface soil water dynamics during dry and wet weather. **(a)** Dry weather soil water dynamics at Schenley are characterized by vertical and lateral flow downslope (straight arrows) and evapotranspiration in surface soils (wavy arrows). **(b)** Wet weather soil water dynamics at Schenley are characterized primarily by bottom-up wetting and slow vertical infiltration in surface soils. **(c)** Dry weather soil water dynamics at Beacon are characterized by vertical and lateral flow downslope in upper layers and evapotranspiration in surface soils, with saturated conditions at depth. **(d)** Wet weather soil water dynamics at Beacon are characterized by top-down wetting and low storm responses in lower soils due to high antecedent soil moisture conditions. (Not to scale).

3.4.2 Implications for Green Infrastructure

Continuous monitoring of soil water dynamics along two urban hillslopes has revealed unexpected hydrological regimes that result in saturated subsurface soils during storm events. In particular, the saturation of these subsurface soils could persist at some sites during drier conditions due to water inputs from bedrock fracture flow. Infiltration-based green infrastructure installed at these sites could experience diminished hydrological function from the high antecedent soil moisture conditions inhibiting a timely redistribution of stormwater to the subsurface.

Infiltration is a dynamic process that is affected by slope, water input rates, and antecedent soil moisture content (Nassif and Wilson, 1975). Drier soils allow for higher infiltration rates due to negative pore pressure pulling water into the soil matrix, and saturated conditions slow infiltration rates due to positive pore pressures exerting force against inflowing water (Dingman, 1994). If lateral fluxes of subsurface soil water downslope are slow due to low hydraulic conductivities, infiltration becomes limited to those hydrologic controls. Studies have found that high antecedent soil moisture conditions led to hydrological failure of infiltration-based green infrastructure for these very reasons (Hardie et al., 2011; Hood et al., 2007; Williams and Wise, 2006). The improper function arose from inhibitions to infiltration and was found to lead to structural overflow (Warnaars et al., 1999) and higher surface runoff at the site than were expected (Penna et al., 2011). The high soil water content of deep soils at Beacon creates a sustained, shallow water table at 60-90 cm below the surface that can lead to decreased hydrologic function of any infiltration systems installed at the site. If groundwater levels were deeper (> 1 m below the bottom of the structure), redistribution of stormwater out of the infiltration structure would be enhanced from vertical and lateral flow infiltration (Figure 3.23a);

however, the shallow water table can inhibit vertical flow, so stormwater will not be able to move away from the infiltration structure as quickly, resulting in decreased infiltration rates near the infiltration structure (Figure 3.23b) (Bouwer, 2002). Although Schenley does not have a shallow water table during dry periods, bottom-up wetting pushes the water table upwards during storm events and can cause similar issues. Currently, short-term drainage after storm events are more rapid at Schenley than at Beacon, but continuous inputs of stored water from green infrastructure could lead to more prolonged saturation and thus lower infiltration rates throughout the soil profile.

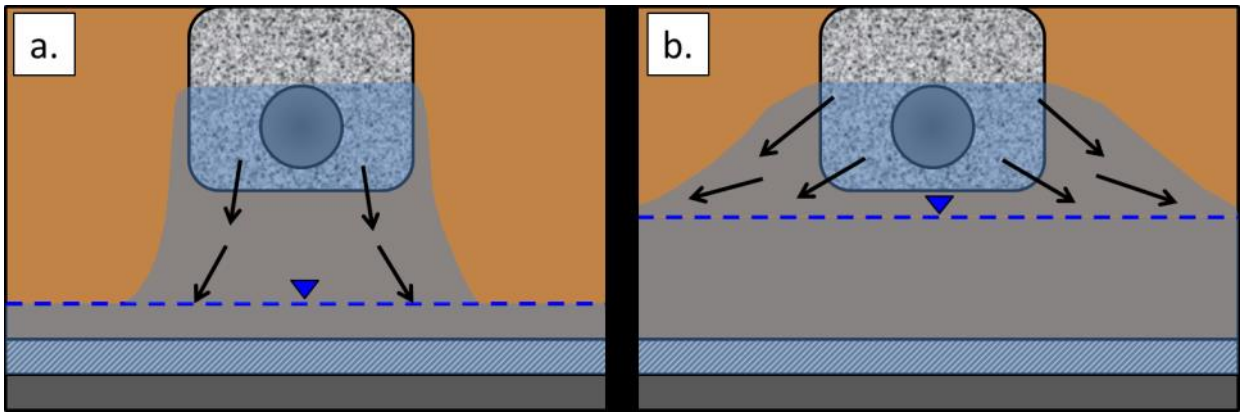

Figure 3.23: Limits to infiltration from groundwater depth. The diagram shows how groundwater depth affects the function of infiltration-based green infrastructure. **(a)** Water can infiltrate vertically and laterally when water tables are deep, but **(b)** vertical infiltration is limited when water tables are shallow (modified from Bouwer 2002).

Without rapid stormwater redistribution, water inputs from green infrastructure at Beacon and Schenley can lead to groundwater mounding (Figure 3.23b), which has been shown to decrease structural integrity of the infiltration device and cause damage to local infrastructure (Endreny and Collins, 2009; Göbel et al., 2004). Groundwater mounding is a particular problem for regions with silty-clay soils with low hydraulic conductivities (Machusick et al., 2011), such

as those found at Beacon and Schenley. In addition, high antecedent soil moisture in the unsaturated zone at the sites will only heighten mounding rates (Göbel et al., 2004). When water tables are shallow, the infiltration devices at the sites will create a feedback loop where groundwater mounding causes decreased infiltration rates in surrounding soils, which will in turn lead to more heightened mounding. In addition to this, infiltration devices are not encouraged for stormwater management in regions with shallow water tables and high antecedent soil moisture (Shuster et al., 2007) because of the risk of contamination of local aquifers from pollutants in the infiltrated stormwater (Pitt et al., 1999).

The less than optimal hydrological conditions at Beacon and Schenley could prevent existing infiltration devices from functioning properly by inhibiting infiltration, promoting groundwater mounding, and increasing risks of groundwater contamination. If other hillslope regions within Pittsburgh have similar soil water dynamics, then infiltration-based green infrastructure may not be the best option for sustainable stormwater management for the city.

3.4.3 Continuous Monitoring as a Site Evaluation Tool

Continuous spatial and temporal monitoring of soil moisture throughout the soil profile can yield more comprehensive interpretations of local soil water dynamics than traditional evaluation tools. Traditional field techniques use soil trenches and infiltration tests to collect site-specific hydrological data, but these methods can only give a representative view of local soil water dynamics by conducting thorough, long-term observations and re-sampling of soils during various dry and wet periods (Barbosa et al., 2012; Tromp-van Meerveld and McDonnell, 2006), but this can be a tedious and costly process. Other studies have shown the importance of continued, site-specific hydrological analyses to properly understand local subsurface processes

and the impacts to green infrastructure (Bronstert and Bardossy, 1999; Shuster et al., 2007). This study agrees well with previous work (Lin and Zhou, 2008) that has shown the applicability of in-situ soil moisture monitoring in understanding soil water dynamics. However, the study is also limited by sampling extent, and interpretations of the hydrological regime may just be a snapshot of a more spatially dynamic system. Previous studies found that soil water dynamics and storm response were strongly dependent on the spatial variation of average antecedent soil moisture across a hillslope, especially during dry seasons (Bachmair and Weiler, 2011; Bronstert and Bardossy, 1999). More accurate predictions of storm response can be made when considering spatial variability of soil moisture (Western et al., 1999); therefore more spatially extended monitoring efforts across hillslopes are needed to clearly understand subsurface soil water dynamics at sites being evaluated for infiltration-based green infrastructure.

The interpretation is also only representative of drier, summer months, but local hydrological regimes experience drastic seasonal changes. In temperate climates like those in Pennsylvania, soils remain saturated throughout the winter months. Cold temperatures and low evapotranspiration rates cause slow lateral flow in the soils and decreases infiltration rates (Bouwer, 2002), leading to higher seasonal water tables. Saturated winter soils experience more frequent runoff events even when infiltration devices are present (Fletcher et al., 2013; Hamel et al., 2013), so winter and spring data should also be collected and analyzed for storm response and effects from snowmelt. Having complete temporal analyses can give insight into implications for infiltration-based green infrastructure year-round.

Data from continuous monitoring of soil moisture can also be used to better design and calibrate models of hillslope subsurface flow to give a more accurate representation of soil water dynamics at that site (Esteves et al., 2000). This can aid in better predictions of green

infrastructure function over time. The most commonly used models for site evaluation are designed as rainfall-runoff models that operate off inputs from local databases and basic field measurements (Fletcher et al., 2013). However, these models would not be able to predict unexpected influences from subsurface soil water processes like those found at our sites without thorough field analyses. Some hydrological models account for the influences of shallow groundwater tables on green infrastructure function, but knowledge from field observations was needed first to predict these dynamics (Jeppesen and Christensen, 2015). In addition, most models are not designed to include water inputs and outputs from bedrock fracture flow (Tromp-van Meerveld and Weiler, 2008), but soil moisture data can reveal if these processes are important to local water balances and can then be reincorporated into the program to create more accurate predictions. Though models can be calibrated with data to more adequately reflect hydrology, these are limited to the quality of the calibration data (Jacobson, 2011). Hamel (2013) suggests that current-day models be optimized through research on long-term, continuous, direct observations of local hydrological conditions, to better predict functionality of infiltration-based green infrastructure. The continuous monitoring methods presented in this study can provide the thorough evaluation of subsurface soil water dynamics that are needed to supplement hydrological models designed to determine long-term functionality of infiltration-based green infrastructure.

4.0 CONCLUSIONS

In urbanized areas, large volumes of stormwater runoff from impervious surfaces can overwhelm sewer systems and be redirected as overflow into local waterways. In cities with antiquated combined sewer systems, these overflow events pose a risk to water quality and public health by delivering both stormwater and waste into receiving waters. Allegheny County, PA, has the largest number of combined sewer overflow inputs in the nation, and is developing a wet weather plan to help mitigate overflow events by implementing innovative stormwater management practices through the use of green infrastructure. Green infrastructure commonly utilizes infiltration systems to convey surface runoff from impervious surfaces into surrounding soils in order to reconnect stormwater to subsurface flow. In order to assess the efficacy of infiltration-based green infrastructure in urban areas of Allegheny County, PA, we explored potential limitations to infiltration from local impervious cover thresholds and from existing subsurface soil water dynamics.

In the first study (see Section 2.0), effective precipitation rates from varying percentages of impervious cover were calculated and compared to locally averaged infiltration rates, with the assumption that storms with effective precipitation rates higher than infiltration rates will generate runoff. In Allegheny County, the effective precipitation of a 1-inch storm surpassed local infiltration rates at 60% impervious cover, which was determined as the impervious cover threshold above which stormwater loading would overwhelm adjacent pervious surfaces. This

suggests that infiltration-based green infrastructure installed in regions with >60% impervious cover would be overwhelmed by stormwater inputs and could degrade infiltration systems via clogging and increased pollutant loading, which also risks contaminating local groundwater. However, more site specific investigations of infiltration rates in these regions can better characterize thresholds within smaller-scale catchments.

The second study (see Section 3.0) used continuous spatial and temporal monitoring of soil moisture content to characterize subsurface soil water dynamics at two hillslope sites (Beacon and Schenley) in Pittsburgh, PA. The Beacon site was found to have high antecedent soil moisture conditions in deep soil layers which could suggest the presence of a shallow water table, and the Schenley site experienced an unexpected bottom-up wetting regime during storm events. Any infiltration-based green infrastructure installed at these sites would experience decreased hydrological function because these conditions decrease infiltration rates of surrounding soils and available water storage for stormwater inputs. More spatially extensive monitoring would be needed to determine the variability of subsurface soil water dynamics across the catchment.

The use of green infrastructure to mitigate stormwater runoff entering local sewer systems is a more sustainable option to the expansion and maintenance of existing grey infrastructure in Allegheny County; however, knowledge gaps in the placement of infiltration systems can lead to poor investment into green infrastructure that is not the best option for that site. The research presented here suggests that infiltration-based green infrastructure may not be the best stormwater management practice for urban areas of Allegheny County due to high probability of early hydrological failure of the systems or groundwater contamination. More thorough site evaluation tools and standards are needed to determine the efficacy of infiltration

systems within geologically and hydrologically unique watersheds. Continuous spatial and temporal monitoring of soil moisture can give a better representation of subsurface soil water dynamics than conventional techniques, and can therefore be used to identify regions that are unsuitable for infiltration of stormwater. In addition, determining local impervious cover thresholds can yield better predictions of catchment-specific limits to infiltration than state or federal standards. These methods will help to avoid improper placement of infiltration-based green infrastructure or to identify regions where these systems will need augmentation with other stormwater management practices.

BIBLIOGRAPHY

3RWW (2001). *Calibrated Radar Rainfall Data*. 3 Rivers Wet Weather. (Pittsburgh, PA) <http://www.3riverswetweather.org/>

ALCOSAN (2008). *Wet Weather Plan: Draft.* Allegheny County Sanitary Authority. (Pittsburgh, PA) <http://alcosan.org/>

Allegheny County (2006). Allegheny County - Street Edge of Pavement. In: "2004 Flyover Base Data". Allegheny County Division of Computer Services Geographic Information Systems Group, Pittsburgh, PA [vector digital data]

Allegheny County (2013a). Allegheny County - Building Footprints. In "2004 Flyover Base Data". Allegheny County Division of Computer Services Geographic Information Systems Group, Pittsburgh, PA. [vector digital data]

Allegheny County (2013b). Allegheny County Imagery 2013. Allegheny County Division of Computer Services Geographic Information Systems Group, Pittsburgh, PA [remote sensing imagery]

Anderson, D. G. (1970). Effects of urban development on floods in northern Virginia. GEOLOGICAL SURVEY WATER-SUPPLY PAPER 2001_C. US Government Printing Office, Washington D.C.

Anderson, S. P., Dietrich, W. E., Montgomery, D. R., Torres, R., Conrad, M. E., and Loague, K. (1997). Subsurface flow paths in a steep, unchanneled catchment. *Water Resources Research* **33**, 2637-2653.

Arnold, C. L., and Gibbons, C. J. (1996). Impervious surface coverage: the emergence of a key environmental indicator. *Journal of the American planning Association* **62**, 243-258.

Arrington, K. E., Ventura, S. J., and Norman, J. M. (2013). Predicting saturated hydraulic conductivity for estimating maximum soil infiltration rates. *Soil Science Society of America Journal* **77**, 748-758.

Bachmair, S., and Weiler, M. (2011). New dimensions of hillslope hydrology. In: *"Forest Hydrology and Biogeochemistry: Synthesis of Past Research and Future Directions"* (D. F. Levia, ed.), pp. 455-481. Springer, Netherlands.

Barbosa, A., Fernandes, J., and David, L. (2012). Key issues for sustainable urban stormwater management. *Water Research* **46**, 6787-6798.

Barnes, J., and Sevon, W. (1996). Educational Series 4: The Geological Story of Pennsylvania. Pennsylvania Geological Survey. (Pittsburgh, PA)

Booth, D. B., Hartley, D., and Jackson, R. (2002). Forest Cover, Impervious-surface Area, and the Mitigation of Stormwater Impacts. *JAWRA Journal of the American Water Resources Association* **38**, 835-845.

Bouwer, H. (2002). Artificial recharge of groundwater: hydrogeology and engineering. *Hydrogeology Journal* **10**, 121-142.

Brander, K. E., Owen, K. E., and Potter, K. W. (2005). Modeled impacts of development type on runoff volume and infiltration performance. *Journal of the American Water Resources Association* **40**, 961-970.

Broadhead, A., Horn, R., and Lerner, D. (2013). Captured streams and springs in combined sewers: a review of the evidence, consequences and opportunities. *Water Research* **47**, 4752-4766.

Bronstert, A., and Bardossy, A. (1999). The role of spatial variability of soil moisture for modelling surface runoff generation at the small catchment scale. *Hydrology and Earth System Sciences Discussions* **3**, 505-516.

Burns, D., Vitvar, T., McDonnell, J., Hassett, J., Duncan, J., and Kendall, C. (2005). Effects of suburban development on runoff generation in the Croton River basin, New York, USA. *Journal of Hydrology* **311**, 266-281.

Burns, M. J., Fletcher, T. D., Walsh, C. J., Ladson, A. R., and Hatt, B. E. (2012). Hydrologic shortcomings of conventional urban stormwater management and opportunities for reform. *Landscape and Urban Planning* **105**, 230-240.

Clark, S. E., Burian, S., Pitt, R., and Field, R. (2007). Urban wet-weather flows. *Water Environment Research* **79**, 1166-1227.

Curriero, F. C., Patz, J. A., Rose, J. B., and Lele, S. (2001). The association between extreme precipitation and waterborne disease outbreaks in the United States, 1948-1994. *American journal of public health* **91**, 1194-1199.

Damodaram, C., Giacomoni, M. H., Prakash Khedun, C., Holmes, H., Ryan, A., Saour, W., and Zechman, E. M. (2010). Simulation of combined best management practices and low impact development for sustainable stormwater management. *Journal of the American Water Resources Association* **46**, 907-918.

Dechesne, M., Barraud, S., and Bardin, J.-P. (2005). Experimental assessment of stormwater infiltration basin evolution. *Journal of environmental engineering* **131**, 1090-1098.

Dietz, M. E. (2007). Low impact development practices: A review of current research and recommendations for future directions. *Water, air, and soil pollution* **186**, 351-363.

Dingman, S. L. (1994). "Physical Hydrology," Prentice Hall, New Jersey.

Endreny, T., and Collins, V. (2009). Implications of bioretention basin spatial arrangements on stormwater recharge and groundwater mounding. *Ecological Engineering* **35**, 670-677.

EPA (2004). Report to Congress on the Impacts and Control of CSOs and SSOs. United States Environmental Protection Agency (Washington, DC)

EPA (2011). Estimating Change in Impervious Area (IA) and Directly Connected Impervious Areas (DCIA) for New Hampshire Small MS4 Permit. United States Environmental Protection Agency. (Washington, DC)

Esteves, M., Faucher, X., Galle, S., and Vauclin, M. (2000). Overland flow and infiltration modelling for small plots during unsteady rain: numerical results versus observed values. *Journal of Hydrology* **228**, 265-282.

Fetter, C. W. (2000). "Applied Hydrogeology", 4th Ed. New Jersey, Prentice Hall.

Field, R., and Struzeski, E. J., Jr (1972). Management and control of combined sewer overflows. *Journal (Water Pollution Control Federation)* **44**, 1393-1415.

Fletcher, T., Andrieu, H., and Hamel, P. (2013). Understanding, management and modelling of urban hydrology and its consequences for receiving waters: A state of the art. *Advances in Water Resources* **51**, 261-279.

Gasperi, J., Gromaire, M.-C., Kafi, M., Moilleron, R., and Chebbo, G. (2010). Contributions of wastewater, runoff and sewer deposit erosion to wet weather pollutant loads in combined sewer systems. *Water Research* **44**, 5875-5886.

Gilroy, K. L., and McCuen, R. H. (2009). Spatio-temporal effects of low impact development practices. *Journal of Hydrology* **367**, 228-236.

Glick, R. H. (2009). Impacts of Impervious Cover and Other Factors on Storm-Water Quality in Austin, Tex. *Journal of Hydrologic Engineering* **14**, 316-323.

Göbel, P., Stubbe, H., Weinert, M., Zimmermann, J., Fach, S., Dierkes, C., Kories, H., Messer, J., Mertsch, V., and Geiger, W. F. (2004). Near-natural stormwater management and its effects on the water budget and groundwater surface in urban areas taking account of the hydrogeological conditions. *Journal of Hydrology* **299**, 267-283.

Graham, C. B., Woods, R. A., and McDonnell, J. J. (2010). Hillslope threshold response to rainfall:(1) A field based forensic approach. *Journal of Hydrology* **393**, 65-76.

Grayson, R. B., Western, A. W., Chiew, F. H., and Blöschl, G. (1997). Preferred states in spatial soil moisture patterns: Local and nonlocal controls. *Water Resources Research* **33**, 2897-2908.

Hamel, P., Daly, E., and Fletcher, T. D. (2013). Source-control stormwater management for mitigating the impacts of urbanisation on baseflow: A review. *Journal of Hydrology* **485**, 201-211.

Hammer, T. R. (1972). Stream channel enlargement due to urbanization. *Water Resources Research* **8**, 1530-1540.

Hardie, M. A., Cotching, W. E., Doyle, R. B., Holz, G., Lisson, S., and Mattern, K. (2011). Effect of antecedent soil moisture on preferential flow in a texture-contrast soil. *Journal of Hydrology* **398**, 191-201.

Harlow, G. E., and LeCain, G. D. (1993). Hydraulic characteristics of, and ground-water flow in, coal-bearing rocks of southwestern Virginia. *United States Geological Survey*. Water-Supply Paper 2388.

Harr, R. D. (1977). Water flux in soil and subsoil on a steep forested slope. *Journal of hydrology* **33**, 37-58.

Hewlett, J. D., and Hibbert, A. R. (1963). Moisture and energy conditions within a sloping soil mass during drainage. *Journal of Geophysical Research* **68**, 1081-1087.

Hollis, G. (1975). The effect of urbanization on floods of different recurrence interval. *Water Resources Research* **11**, 431-435.

Holman-Dodds, J. K., Bradley, A. A., and Potter, K. W. (2003). Evaluation of hydrologic benefits of infiltration based urban storm water management. *Journal of the American Water Resources Association* **39**, 205-215.

Hood, M. J., Clausen, J. C., and Warner, G. S. (2007). Comparison of Stormwater Lag Times for Low Impact and Traditional Residential Development1. *JAWRA Journal of the American Water Resources Association* **43**, 1036-1046.

Hopkins, K. G., Bain, D. J., and Copeland, E. M. (2014). Reconstruction of a century of landscape modification and hydrologic change in a small urban watershed in Pittsburgh, PA. *Landscape Ecology* **29**, 413-424.

Jacobson, C. R. (2011). Identification and quantification of the hydrological impacts of imperviousness in urban catchments: A review. *Journal of Environmental Management* **92**, 1438-1448.

Jeppesen, J., and Christensen, S. (2015). A MODFLOW Infiltration Device Package for Simulating Storm Water Infiltration. *Groundwater* **53**, 542-549.

Kaushal, S. S., and Belt, K. T. (2012). The urban watershed continuum: evolving spatial and temporal dimensions. *Urban Ecosystems* **15**, 409-435.

Kirk, B. (2014). Personal communication via e-mail. [excel spreadsheet]

Klein, R. D. (1979). Urbanization and stream quality impairment. *Water Resources Bulletin* **15**, 948-963.

Kozar, M. D., McCoy, K. J., Britton, J. Q., and Blake Jr., B. M. (2012). Hydrogeology, Groundwater Flow, and Groundwater Quality of an Abandoned Underground Coal-Mine Aquifer, Elkhorn Area, West Virginia. U.S. Geological Survey. Bulletin B-46.

Le Coustumer, S., Fletcher, T. D., Deletic, A., Barraud, S., and Lewis, J. F. (2009). Hydraulic performance of biofilter systems for stormwater management: influences of design and operation. *Journal of hydrology* **376**, 16-23.

Leopold, L. B. (1968). Hydrology for urban land planning: A guidebook on the hydrologic effects of urban land use. U.S. Geological Survey Circular 554.

Lin, H., and Zhou, X. (2008). Evidence of subsurface preferential flow using soil hydrologic monitoring in the Shale Hills catchment. *European Journal of Soil Science* **59**, 34-49.

Loperfido, J. V., Noe, G. B., Jarnagin, S. T., and Hogan, D. M. (2014). Effects of distributed and centralized stormwater best management practices and land cover on urban stream hydrology at the catchment scale. *Journal of Hydrology* **519**, 2584-2595.

Machusick, M., Welker, A., and Traver, R. (2011). Groundwater mounding at a storm-water infiltration BMP. *Journal of Irrigation and Drainage Engineering* **137**, 154-160.

McMahon, G., Bales, J. D., Coles, J. F., Giddings, E. M., and Zappia, H. (2003). Use of stage data to characterize hydrologic conditions in an urbanizing environment. *Journal of the American Water Resources Association* **39**, 1529-1546.

Meliora (2011). Restoring the health of panther hollow: A plan for watershed Restoration. Pittsburgh Parks Conservancy, Meliora Environmental Design. (Philadelphia, PA)

Mikkelsen, P. S., Jacobson, P., and Fujita, S. (1996). Infiltration practice for control of urban storm water. *Journal of Hydraulic Research* **34**, 827-840.

Moglen, G. E., and Kim, S. (2007). Limiting imperviousness: are threshold-based policies a good idea? *Journal of the American Planning Association* **73**, 161-171.

Mohanty, B., Skaggs, T. H., and Famiglietti, J. (2000). Analysis and mapping of field-scale soil moisture variability using high-resolution, ground-based data during the Southern Great Plains 1997 (SGP97) Hydrology Experiment. *Water Resources Research* **36**, 1023-1031.

Montgomery, D. R., Dietrich, W. E., Torres, R., Prestrud Anderson, S., Heffner, J. T., and Loague, K. (1997). Hydrologic response of a steep, unchanneled valley to natural and applied rainfall. *Water Resources Research* **33**, 91-109.

Nassif, S., and Wilson, E. (1975). THE INFLUENCE OF SLOPE AND RAIN INTENSITY ON RUNOFF AND INFILTRATION/L'influence de l'inclinaison de terrain et de l'intensité de pluie sur l'écoulement et l'infiltration. *Hydrological Sciences Journal* **20**, 539-553.

Newbury, R. L., Belz, D. J., and Grubb, R. G. (1981). Soil Survey of Allegheny County, Pennsylvania. USDA Soil Conservation Service.

NRCS (1987). Module 3 - USDA Textural Soil Classification. In: *Soil Mechanics Level 1: Study Guide*. Natural Resources Conservation Service.

NWS (2013). 1981-2010 Climate Normals, Pittsburgh, Pennsylvania. NOAA National Weather Service, Accessed: Jan. 2015.

Onda, Y., Komatsu, Y., Tsujimura, M., and Fujihara, J.I. (2001). The role of subsurface runoff through bedrock on storm flow generation. *Hydrological Processes* **15**, 1693-1706.

PADEP (2006). Pennsylvania Stormwater Best Management Practices Manual. Pennsylvania Department of Environmental Protection; Bureau of Watershed Management.

PASDA (2013). Pennsylvania Spatial Data Access. Pennsylvania State University; Pennsylvania Office for Information Technology. [geospatial data] <http://www.pasda.psu.edu/>

Paul, M. J., and Meyer, J. L. (2001). Streams in the urban landscape. *Annual Review of Ecology and Systematics* **32**, 333-365.

Penna, D., Borga, M., Norbiato, D., and Dalla Fontana, G. (2009). Hillslope scale soil moisture variability in a steep alpine terrain. *Journal of Hydrology* **364**, 311-327.

Penna, D., Tromp-van Meerveld, H., Gobbi, A., Borga, M., and Dalla Fontana, G. (2011). The influence of soil moisture on threshold runoff generation processes in an alpine headwater catchment. *Hydrology and Earth System Sciences* **15**, 689-702.

Perez-Pedini, C., Limbrunner, J. F., and Vogel, R. M. (2005). Optimal location of infiltration-based best management practices for storm water management. *Journal of Water Resources, Planning, and Management* **131**, 441-448.

Pitt, R., Clark, S., and Field, R. (1999). Groundwater contamination potential from stormwater infiltration practices. *Urban Water* **1**, 217-236.

PWSA (2013). PWSA Wet Weather Feasibility Study. Pittsburgh Water and Sewer Authority. (Pittsburgh, PA)

Qiu, Y., Fu, B., Wang, J., and Chen, L. (2001). Soil moisture variation in relation to topography and land use in a hillslope catchment of the Loess Plateau, China. Journal of Hydrology **240**, 243-263.

R Core Team (2013). R: A language and environment for statistical computing. R Foundation for Statistical Computing. (Vienna, Austria)

Reddi, L. N., Ming, X., Hajra, M. G., and Lee, I. M. (2000). Permeability reduction of soil filters due to physical clogging. *Journal of Geotechnical and Geoenvironmental Engineering* **126**, 236-246.

Robinson, D., Campbell, C., Hopmans, J., Hornbuckle, B., Jones, S. B., Knight, R., Ogden, F., Selker, J., and Wendroth, O. (2008). Soil moisture measurement for ecological and hydrological watershed-scale observatories: A review. *Vadose Zone Journal* **7**, 358-389.

Rose, S., and Peters, N. E. (2001). Effects of urbanization on streamflow in the Atlanta area (Georgia, USA): a comparative hydrological approach. *Hydrological Processes* **15**, 1441-1457.

Roy, A. H., and Shuster, W. D. (2009). Assessing impervious surface connectivity and applications for watershed management1. *JAWRA Journal of the American Water Resources Association* **45**, 198-209.

Schueler, T. R. (1994). The importance of imperviousness. *Watershed Protection Techniques* **1**, 100-111.

Seaber, P. R., Brahana, J., and Hollyday, E. (1988). Region 20, Appalachian plateaus and valley and ridge. *In* "The Geology of North America", Vol. O-2, Hydrogeology, pp. 189-200. The Geological Society of America.

Semadeni-Davies, A., Hernebring, C., Svensson, G., and Gustafsson, L.-G. (2008). The impacts of climate change and urbanisation on drainage in Helsingborg, Sweden: Combined sewer system. *Journal of Hydrology* **350**, 100-113.

Sheets, C. J., and Kozar, M. D. (2000). Ground-Water Quality in the Appalachian Plateaus, Kanawha River Basin, West Virginia. National Water-Quality Assessment Program, US Geological Survey. Water-Resources Investigations Report 99-4269.

Shuster, W., Bonta, J., Thurston, H., Warnemuende, E., and Smith, D. (2005). Impacts of impervious surface on watershed hydrology: A review. *Urban Water Journal* **2**, 263-275.

Shuster, W., Gehring, R., and Gerken, J. (2007). Prospects for enhanced groundwater recharge via infltration of urban storm water runoff: A case study. *Journal of Soil and Water Conservation* **62**, 129-137.

Soil Survey Staff (2014). National Resources Conservation Services, United States Department of Agriculture. Web Soil Survey. < http://websoilsurvey.sc.egov.usda.gov>

Takagi, K., and Lin, H. (2012). Changing controls of soil moisture spatial organization in the Shale Hills Catchment. *Geoderma* **173-174**, 289-302.

Tarr, J. A. (2004). "Devastation and renewal: an environmental history of Pittsburgh and its region," University of Pittsburgh Press, Pittsburgh, PA.

Tromp-van Meerveld, H., and McDonnell, J. (2006). On the interrelations between topography, soil depth, soil moisture, transpiration rates and species distribution at the hillslope scale. *Advances in Water Resources* **29**, 293-310.

Tromp-van Meerveld, I., and Weiler, M. (2008). Hillslope dynamics modeled with increasing complexity. *Journal of Hydrology* **361**, 24-40.

Tromp-van Meerveld, H., and McDonnell, J. (2006). Threshold relations in subsurface stormflow: (1) A 147-storm analysis of the Panola hillslope. *Water Resources Research* **42**, W02410.

Tromp-van Meerveld, H., Peters, N., and McDonnell, J. (2007). Effect of bedrock permeability on subsurface stormflow and the water balance of a trenched hillslope at the Panola Mountain Research Watershed, Georgia, USA. *Hydrological Processes* **21**, 750-769.

Tsujimura, M., Onda, Y., Fujiwara, J., and Ito, J. (1999). Hydrometric and tracer approaches to investigate rainfall-runoff processes in mountainous basins with different geologies. *Integrated Methods in Catchment Hydrology: Tracer, Remote Sensing and New Hydrometric Techniques* **IAHS PUBLICATION No. 258**, 159-166.

Uchida, T., Asano, Y., Ohte, N., and Mizuyama, T. (2003). Seepage area and rate of bedrock groundwater discharge at a granitic unchanneled hillslope. *Water Resources Research* **39**, SBH 9: 1-12.

Uchida, T., McDonnell, J. J., and Asano, Y. (2006). Functional intercomparison of hillslopes and small catchments by examining water source, flowpath and mean residence time. *Journal of Hydrology* **327**, 627-642.

USGS (2014). NLCD 2011 Percent Developed Imperviousness (2011 Edition). U.S. Geological Survey, Sioux Falls, SD. [raster digital data]

Wagner, W. R. (1970). Geology of the Pittsburgh Area. *General Geology Report 59*. Commonwealth of Pennsylvania: Department of Internal Affairs, Bureau of Topographic and Geological Survey.

Walsh, C. J., Roy, A. H., Feminella, J. W., Cottingham, P. D., Groffman, P. M., and Morgan, R. P. (2005). The urban stream syndrome: current knowledge and the search for a cure. *Journal of the North American Benthological Society* **24**, 706-723.

Warnaars, E., Larsen, A. V., Jacobsen, P., and Mikkelsen, P. S. (1999). Hydrologic behaviour of stormwater infiltration trenches in a central urban area during 2¾ years of operation. *Water Science and Technology* **39**, 217-224.

Weiler, M., McDonnell, J. J., Tromp-van Meerveld, I., and Uchida, T. (2005). Subsurface Stormflow. *In* "Encyclopedia of Hydrological Sciences" (M. G. Anderson, ed.). John Wiley & Sons, Ltd, New Jersey.

Weiss, P. T., LeFevre, G., and Gulliver, J. S. (2008). "Contamination of Soil and Groundwater Due to Stormwater Infiltration Practices, A Literature Review," University of Minnesota: St. Anthony Falls Laboratory, Minneapolis, Minnesota.

Western, A. W., Grayson, R. B., Blöschl, G., Willgoose, G. R., and McMahon, T. A. (1999). Observed spatial organization of soil moisture and its relation to terrain indices. *Water Resources Research* **35**, 797-810.

Williams, E. S., and Wise, W. R. (2006). Hydrologic impacts of alternative approaches to storm water management and land development. *Journal of the American Water Resources Association* **42**, 443–455.

Wobschall, D. (1978). A frequency shift dielectric soil moisture sensor. *Geoscience Electronics, IEEE Transactions on* **16**, 112-118.

Wolman, M. G. (1967). A cycle of sedimentation and erosion in urban river channels. *Geografiska Annaler. Series A. Physical Geography* **49**, 385-395.

Yeakley, J. A., Swank, W., Swift, L., Hornberger, G., and Shugart, H. (1998). Soil moisture gradients and controls on a southern Appalachian hillslope from drought through recharge. *Hydrology and Earth System Sciences* **2**, 41-49.